Florida A & M University - Florida State University
College of Engineering

Department of Civil & Environmental Engineering

TIME DEPENDENT COMPRESSIVE STRENGTH AND MODULUS OF ELASTICITY OF FLORIDA CONCRETE

By

Nur Yazdani, Ph.D., P.E.
Professor

S. Bryant Mckinnie
Research Assistant

FDOT Contract No. BD-221

Final Report Submitted to the
Florida Department of Transportation

March 2004

TECHNICAL REPORT DOCUMENTATION PAGE

1. Report No.	2. Government Accession No.	3. Recipient's Catalog No.
4. Title and Subtitle **Time Dependent Strength and Elasticity Development in Florida Concrete**		5. Report Due **March 15, 2004** 6. Performing Organization Code **11-1902-157**
7. Author's **Nur Yazdani, Ph.D., P.E., S. Bryant Mckinnie**		8. Performing Organization Report No. **11-1902-157**
9. Performing Organization Name and Address **FAMU-FSU College of Engineering** **Civil and Environmental Engineering Department** **2525 Pottsdamer St.** **Tallahasse FL 32310**		10. Work Unit No. (TRAIS) 11. Contract or Grant No. **BD-221**
12. Sponsoring Agency Name and Address **Florida Department of Transportation** **605 Suwannee Street** **Tallahassee, FL 32399-0450**		13. Type of Report and Period Covered **Final Report** 14. Sponsoring Agency Code
15. Supplementary Notes		

16. Abstract

The Florida Department of Transportation (FDOT) requirements for concrete compressive strength may be met through drilled core specimen testing, and prediction of an equivalent 28-day compressive strength based on the core strength. The equivalent compressive strengths meeting the specified FDOT requirements are acceptable; specimens that fall below the specified strength are used to determine an appropriate pay reduction. The current FDOT pay reduction equations have been used for many years, and may not represent current FDOT concrete. Compressive strength testing using a typical FDOT Class IV mix design at various ages was performed herein in order to develop time dependent compressive strength variation models. The test matrix was based on the substitution of cement types (I, II and III), fly ash (with slag) and coarse aggregate types (Calera, river gravel and Brooksville). Statistical analysis was applied to the compressive strength data from these tests to develop new strength prediction models. The various resulting models were compared to the current FDOT pay reduction models and to each other, and the best models were selected.

The current FDOT concrete modulus of elasticity (MOE) empirical model is a function of concrete compressive strength and unit weight. Recent testing shows that this model consistently underestimates the MOE for FDOT concrete. This underestimation may lead to construction problems caused by over-prediction of camber and deflection of concrete structural members. MOE values were experimentally determined at various concrete ages for the typical concrete mixes used previously. Regression analyses were used to find the best fit MOE models to the generated data, and such models were compared with existing MOE models from the literature. It was found that the aggregate type and specific gravity plays a significant role in influencing concrete MOE. Best fit MOE models for FDOT concrete together with suggested modifiers for various aggregate types were recommended.

17. Key Words	18. Distribution Statement
Concrete compressive strength, time-dependent variation, modulus of elasticity, pay reduction	**No restriction** **This report is available to the public through the National Technical Information Service, Springfield VA 22161**

19. Security Classif. (of this report)	20. Security Classif. (of this page)	21. No. of Pages	22. Price
Unclassified	**Unclassified**	**127**	

Form DOT F 1700.7 (8-72)

Reproduction of completed page authorized

TABLE OF CONTENTS

LIST OF TABLES

LIST OF FIGURES

ABSTRACT

The Florida Department of Transportation (FDOT) requirements for concrete compressive strength may be met through drilled core specimen testing, and estimation of an equivalent 28-day compressive strength based on the core strength. The equivalent compressive strengths meeting the specified FDOT requirements are acceptable based on the established correlation; low strength concrete based on its structural evaluation may be accepted with reduced payment. The current FDOT compressive strength correlation equations for pay reduction have been used for many years, and may not represent current FDOT concrete. Compressive strength testing using a typical FDOT Class IV mix design at various ages was performed herein in order to develop time dependent compressive strength variation models. The test matrix was based on the substitution of the original type II cement with types I and III cements. Additional mixes were generated by the substitution of fly ash with slag, and the original Brooksville aggregate with River Gravel and Calera aggregates. Statistical analysis was applied to the compressive strength data from these tests to develop new strength prediction models. The various resulting models were compared to the current FDOT strength reduction models and to each other, and the best models were selected.

The current FDOT concrete modulus of elasticity (MOE) empirical model is a function of concrete compressive strength and unit weight. Recent testing shows that this model consistently underestimates the MOE for FDOT concrete. This underestimation may lead to construction problems caused by over-prediction of camber and deflection of concrete structural members. MOE values were experimentally determined at various concrete ages for the typical concrete mix used previously. Regression analyses were used to find the best fit MOE models to the generated data, and such models were compared with existing MOE models from the literature. It was found that the aggregate type and specific gravity plays a significant role in influencing concrete MOE. Best fit MOE models for FDOT concrete together with suggested modification factors for various aggregate types were recommended.

CHAPTER 1

INTRODUCTION

1.1 Time-Dependent Variation of Compressive Strength

Concrete used in the Florida Department of Transportation (FDOT) projects must satisfy compressive strength, target slump, and air content requirements, according to FDOT Standard Specifications for Road and Bridge Construction [FDOT 2004]. FDOT concrete is categorized in several classes depending on the intended use of the concrete. FDOT specifications section 346-3.1, Table 2, provides minimum acceptable 28-day compressive strengths, target slumps and air content ranges for various classes of concrete. For each LOT, defined in FDOT Specifications section 346-10, the compressive strength test is determined as the average of the strengths from three test cylinders. If a concrete strength acceptance test falls more than 10% or 500 psi below the specified minimum strength, one option for the contractor is to perform a structural analysis indicating adequate structural strength and durability. The other more commonly utilized alternative is to take drilled core samples to determine in-place compressive strength of the concrete. If cores are tested, the core strength test results are acceptable in lieu of the unacceptable 28-day concrete test cylinder strength of the concrete in question.

[ ] indicates a reference

FDOT may accept concrete that has 28-day compressive strength results less than 10% or 500 psi below the specified minimum strength, if it is otherwise acceptable. However, payment for such low strength concrete is reduced according to FDOT Specifications section 346-11. If cores are not supplied by the contractor, the pay reduction is based on the 28-day strengths from sample cylinders. For cores tested no later than 42 days after concrete casting, FDOT accepts the core strengths to represent the equivalent 28-day compressive strength of the questionable concrete. For cores tested later than 42 days after concrete casting, equivalency must be established between the 28-day compressive strength and the strength after 42 days. FDOT Specifications Section 346-11.6 provides relationships to determine this equivalency, as well as the method of pay reduction for concrete with inadequate compressive strength. These relationships are presented in Section 2.5.1, Eqs. 2.3 through 2.6 of this report.

According to the State Materials office personnel, the FDOT pay reduction formulae for concrete compressive strength are based on studies performed at the Bureau of Reclamation approximately 25 to 30 years ago. Since that time, concrete and concrete technology has changed and improved considerably. In addition to cement, materials such as fly ash, slag and silica fume are now routinely added to FDOT concrete. This leads to improved corrosion protection, improved sulfate resistance and reduced heat of hydration. The specified minimum compressive strength of FDOT concrete has increased to 8,500 psi for Class VI concrete. In addition, admixtures such as water reducers, plasticizers, air entrainers and corrosion inhibitors are routinely added to the concrete mix as admixtures to improve quality. It is apparent that the FDOT concrete of today is much improved and different than the time when the FDOT pay reduction relationships were formulated. As a result, the formulae may or may not accurately assess the quality of concrete or make accurate predictions for pay penalties.

One of the two major objectives of this study was to develop models to accurately reflect the time dependent variation of compressive strength of current Florida concrete. Based on these models, realistic equivalencies for 28-day concrete strengths based on core and cylinder tests and accurate pay reduction relationships can be developed.

1.2 Modulus of Elasticity

Modulus of Elasticity (MOE) of concrete is needed for deflection, camber and stiffness calculations of various structural elements at various time intervals. The FDOT Structures Design Guidelines Section 4.1 mandates the use of Eq. 5.4.2.4-1 of the AASHTO LRFD Bridge Design Specifications [AASHTO 2003] for prediction of MOE, and 90% of this calculated value when Florida lime rock is used as the coarse aggregate. The FDOT MOE equation for Florida lime-rock concrete is as follows:

$$E_c = 30 \cdot w^{1.5} \cdot \sqrt{f'_c} \tag{1.1}$$

where:

E_c = Modulus of Elasticity (psi)

w = unit weight of concrete (pcf)

f'c = compressive strength of concrete (psi)

The ACI and the FDOT MOE equations are reproduced as Eqs. 2.2 and 2.7 in Ch. 2 of this report. Recent limited investigations have shown that the FDOT MOE relationships consistently underestimate the MOE of actual test data for Florida concrete [Cook 1989, 2004]. This may result in inaccurate prediction of deflections and cambers by FDOT design procedures and software, which may lead to construction problems in the field. The MOE values at various time intervals are important for predicting the serviceability of concrete members, especially prestressed concrete. In prestressed concrete members, the behavior at prestress release, at transport of members and in service is of concern.

The other major objective of this study was to develop more accurate equations to predict the MOE for FDOT concrete. This will lead to more accurate prediction of deflection and camber in structural members, resulting in the minimization of construction and serviceability problems. The variation of the concrete MOE at various time intervals may also be helpful in proper prediction of serviceability parameters at different loading stages.

CHAPTER 2

BACKGROUND REVIEW

2.1 Hydraulic Cement & the Structure of Concrete

Hydraulic cements are compound combinations that react chemically with water to harden and develop bonding properties. The primary type of hydraulic cement is Portland cement and is most commonly used in combination with a certain amount of fine and coarse aggregate to form a heterogeneous composite construction material known as concrete. The fine and coarse aggregate are added as less expensive fillers. Portland cement is composed primarily of calcium silicates, calcium aluminates and a small amount of gypsum. Common sources of calcium for this cement are naturally occurring calcium carbonate materials such as limestone, chalk, marl and seashells with clay and dolomite as impurities. Shales and clays containing alumina, iron oxide and alkalis are used as principal sources of silica to combine with the calcium in the manufacturing process. The precise proportions of the raw materials are predetermined for the particular type of cement to be produced. The materials are then well mixed, crushed and pulverized to mostly less than 75 mm particles. After pulverization, the material mixture is rotated through a kiln and heated to approximately 2700°F where the chemical reactions occur between the raw materials to form clinker. Finally, Portland cement is formed when the clinker is ground into particles mostly smaller than 75 mm diameter. Table 2.1 shows the five basic ASTM cement types with typical percentages of their major ingredients, typical fineness displayed as air permeability specific surface, and primary characteristics and uses for each [Mehta 1986, ACI 225R-99]. Cement becomes more reactive with finer particle size, which means it will achieve its strength more quickly and produce a higher heat of hydration. Increased amounts of finer particles provide Type III (high early strength) cement its high early strength. Besides particle size, the rate of reaction between Portland cement compounds and water is influenced by their crystalline structures.

The hydration process is initially controlled by the aluminates because they react first with water to cause the initial setting of the mix. This reaction would be immediate and thereby make the mix useless for construction purposes if gypsum was not present in the cement. Usually the first crystal to form in the reaction is calcium sulfoaluminate, commonly known as ettringite, due to a high sulfate to aluminate ratio in the solution phase during the first hour of hydration. Precipitation of ettringite contributes to the stiffening, setting, and early strength of the mix. Eventually the final product of the aluminates, including ettringite, is the more stable compound monosulfate.

Figure 2.1 shows a graphical representation of the relative volume changes of the various cement components present at different stages of the concrete curing process for the first 28 days. This is a general representation and the relative values would be different for different cement types and curing conditions [ACI 225R-99].

Table 2.1: Chemical & Physical Properties of Cement Types [Mehta 1986, ACI 225R-99]

ASTM Cement Type	C_3S (%)	C_2S (%)	C_3A (%)	C_4AF (%)	Air permeability specific surface (m^2/kg)	(ft^2/lbm)	Description
I	42-65	10-30	0-17	6-18	300-400	1470-1950	General purpose
II	35-60	15-35	0-8	6-18	280-380	1370-1860	General purpose with moderate sulfate resistance and heat of hydration
III	45-70	10-30	0-15	6-18	450-600	2200-2930	High early strength
IV	20-30	50-55	3-6	8-15	280-320	1370-1560	Low heat of hydration
V	40-60	15-40	0-5	10-18	290-350	1420-1710	High sulfate resistance

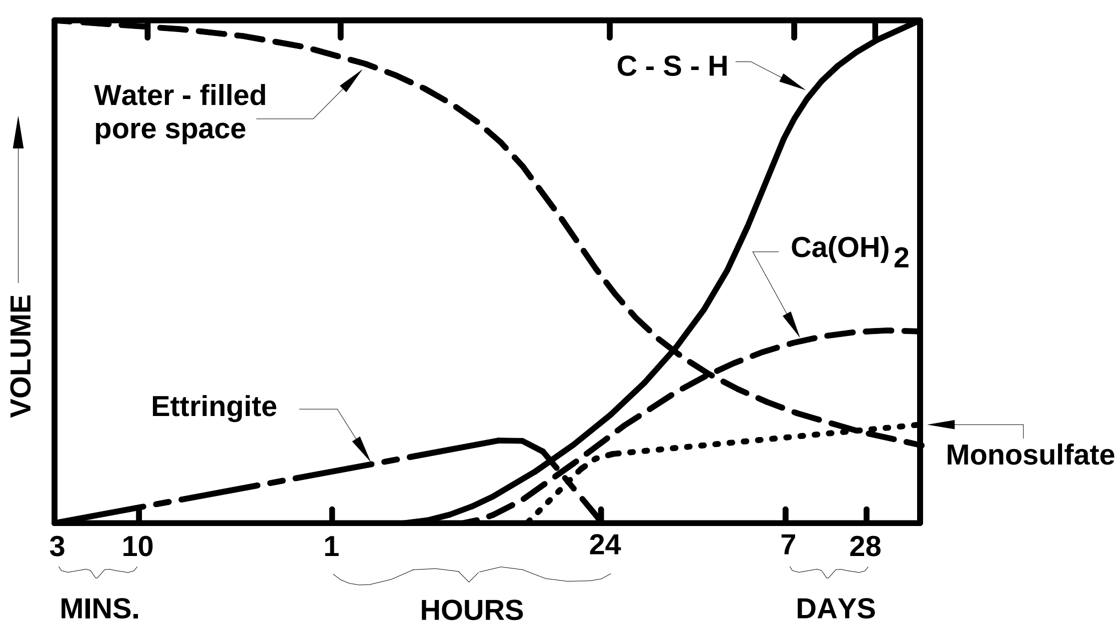

Figure 2.1: Chemical Reactions in Concrete Versus Time of Curing [ACI 225R-99]

There is a trade off between early strength attainment and decreased durability. The finer particle cements such as Type III also cure faster due to more rapid hydration of the smaller particles. This increases the rate of heat production in the concrete, which helps to increase the immediate rate of curing, but has a detrimental effect on the ultimate strength of the concrete [Mehta 1986].

Temperature plays a major role on the rate and manner of concrete strength gain. The maturity method of estimating concrete strength based on a specimen's temperature-time history assumes that increasing the concrete curing temperature accelerates the process. Concrete cured under a lower temperature for a longer period of time would have similar strength gain [ASTM C 1074-98, ASTM C 918-02, Carino and Malhotra 1991]. In general, increases in curing temperature increase the short-term strength of concrete by accelerating the chemical reactions of hydration. However, increases in early age temperature also reduce the ultimate strength, as shown in Fig. 2.2 [Mehta 1986]. This reduction in ultimate strength is due to the fact that higher temperature curing results in a less uniform microstructure and poor pore distribution. Dr. Kevin Rens of the University of Colorado at Denver is currently conducting an experimental study intended to modify and improve the Maturity Method [ASTM C 1074-98]. This study will account for the negative impact of high early age temperature on the ultimate strength of concrete and provide a more accurate prediction of concrete strength [Rens 2004].

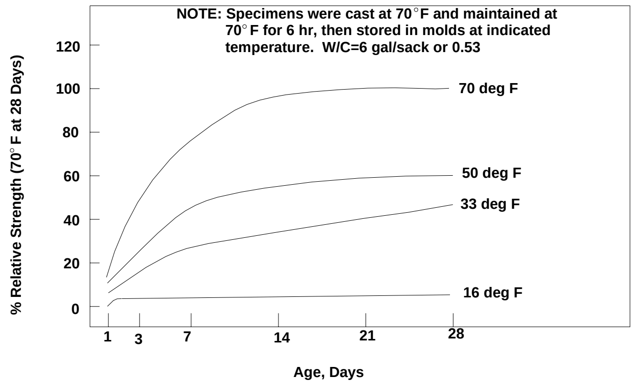

(a) Cured in Molds at 70 °F for the First 6 Hours

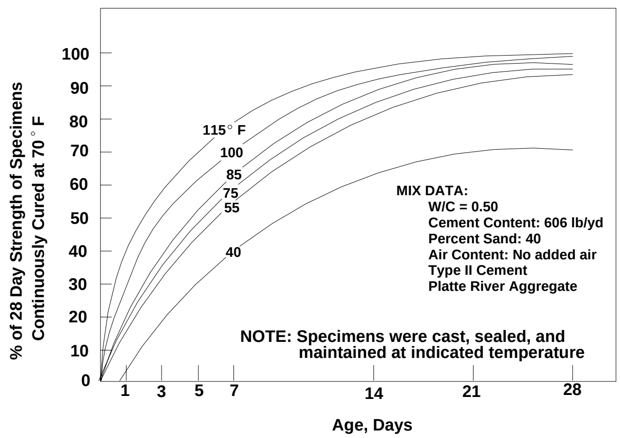

(b) Cast, Sealed and Maintained at Constant Temperature

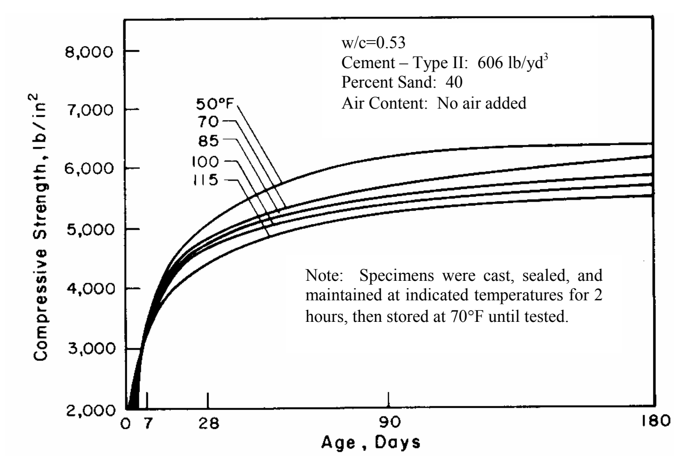

(c) Stored at Indicated Temperature for the First 2 Hours

Figure 2.2: Concrete Strength Gain for Different Curing Temperatures [Mehta 1986]

2.2 Concrete Compressive Strength

The most common and widely known factor affecting concrete compressive strength is the water to cementitious materials ratio (w/c ratio). This is the weight of the water divided by the weight of all cementitious materials (including mineral admixtures) combined. Duff Abrams found the relation know as Abram's water-cement ratio rule expressed as [Mehta 1986]:

$$f'_c = \frac{k_1}{k_2^{(w/c)}} \tag{2.1}$$

where:

f'_c = concrete compressive strength (psi)

k_1, k_2 = empirical constants

w/c = water/cementitious ratio

The compressive strength increases with a decrease in w/c ratio. The thin layer of hydraulic cement paste (HCP) around the surface of the aggregate is called the transition zone. Excess bleed water from the HCP accumulates here and yields a weaker paste locally. This zone is weaker than the bulk HCP because higher water content here means a higher local w/c ratio. The typical mode of failure of a concrete cylindrical specimen under uniaxial compression is through a failure by cracking that initiates in the weaker transition zone, and then propagates through the rest of the HCP. By comparison, in high strength concrete, the mode of failure is a crack through the coarse aggregate and HCP because the strength of the HCP is close to or even exceeds that of the aggregate.

Typically, the larger the coarse aggregate size, more bleed water accumulates in the transition zone, resulting in a weaker concrete matrix. This effect is most predominant in higher strength concrete. However, this effect may be partially offset by the larger aggregate concrete requiring less water for a given workability, and a lower w/c ratio. In addition to size, the surface texture and shape of the coarse aggregates influence the compressive strength. Most coarse aggregates that have a good track record of performance typically do not cause significant bleed water problems [ACI 221R-96].

Sufficient water is required throughout the curing process to ensure proper and complete cement hydration. Theoretically, complete hydration is never actually achieved. However, the early stages of curing are the most critical for moisture to be present in order to gain sufficient strength. Cylinders used in the ASTM 28-day compressive strength test are submerged in water for the entire 28 days of curing [ASTM C 39-03]. The 28-day compressive strength of dry cured specimens can be as much as 45% less than moist cured samples. Therefore, it is very important for concrete to undergo proper moist curing for at least the first several days by wet burlap coverings or sprayed curing compounds to prevent moisture loss [Mehta 1986].

2.3 Chemical and Mineral Admixtures

Chemical admixtures are typically categorized as air entraining, water reducing, high range water reducing, retarding, and accelerating additives or some combination of these. ASTM C 494-04 specifications describe the individual admixture types, as shown in Table 2.2.

Table 2.2: Chemical Admixtures [ASTM C 494-04 and ASTM C 260-01]

Type	Description
A	Water Reducing
B	Retarding
C	Accelerating
D	Water Reducing & Retarding
E	Water Reducing & Accelerating
F	Water Reducing, High Range (HRWR)
G	Water Reducing, High Range, & Retarding
AEA	Air Entraining Admixture

Air entrainment is important for durability and freeze-thaw resistance of concrete. Air entrainment typically reduces the required w/c ratio; however, this may lead to decreased strength. Water reducing admixtures increase the consistency of concrete without addition of water, generally by providing an ionic charge on the surface of the cement particles causing them to repel each other, thereby making the mix more flowable. Larger amounts of water-reducer can retard set time and act as a retarder as well. Even with this set time retardation, early strength gain may be accelerated due to better dispersion of cement particles in the water. High range water reducers, also known as superplasticizers, can reduce water requirements by as much as 20 to 25%, compared to water-reducers which can reduce water requirement by 5 to 10%. Superplasticizers cause less set-time retardation, as compared to water-reducers. Many superplasticizers have an accelerating effect on concrete.

Many current Portland cement mixes use finely divided siliceous materials known as mineral admixtures such as fly ash and slag. These mineral admixtures help reduce the cost of the mix and are used for making durable concrete.

Ground granulated blast-furnace slag is made by pulverizing the rapidly cooled waste products from cast iron production. It is a pozzolanic material, which means it can react with water to form cementing products without the presence of other compounds. The presence of cement accelerates the pozzolanic properties of slag.

Fly ash is the ash waste in the flue gas by-product from the combustion of powdered coal in power plants. High calcium fly ash contains between 15 and 35% CaO, whereas low calcium fly ash contains less than 10% CaO. Low calcium fly ash is pozzolanic, which means it reacts with CH and water to form cementitious products. High calcium fly ash is both pozzolanic and cementitious, which means it can form some cementing products with only the addition of water.

Both blast furnace slag and high calcium fly ash contribute to the ultimate compressive strength and the 28-day compressive strength (Fig. 2.3). Low calcium fly ash does contribute to the ultimate compressive strength of concrete, but this benefit generally does not initiate until sometime after four weeks of curing, and in fact, generally reduces the 7-day and 28-day compressive strengths (Fig. 2.4) [Mehta 1986].

Fly ash and slag reduce the required w/c ratio for a given slump and workability, thereby improving strength if a lower w/c ratio is used. They are cheaper than Portland cement and are cost effective fillers. However, these admixtures also have other benefits beyond reduced cost and increased ultimate strength. The mineral admixtures improve resistance to sulfate and acid attack, and reduce permeability. Because their chemical reactions are generally slow, the heat of hydration is typically reduced. As with cement, the particle size, chemical structure, and stability of fly ash and slag also affect reactivity and curing rates.

ASTM C 618-03 specifications classify fly ash as N, F, or C. This classification is based on the chemical composition of the fly ash and is not intended to address its nature or reactivity. Class C fly ash generally has higher than 20% CaO which causes it to be highly cementitious [ACI 232.2R-96]. Class F fly ash is mostly obtained as the byproduct of burning anthracite or bituminous coal [Mehta 1986]. Class N fly ash, which

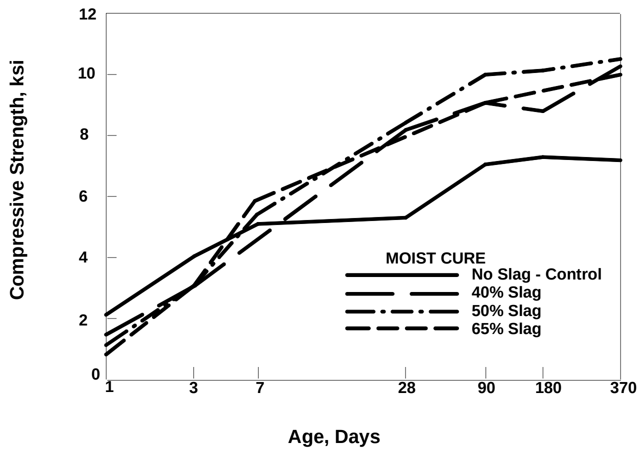

Figure 2.3: Slag Effect on Concrete Compressive Strength [Mehta 1986]

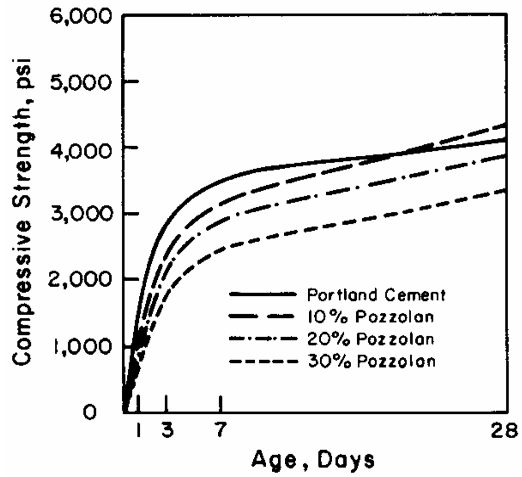

(a) Pozzolan Concrete Through 28 Days

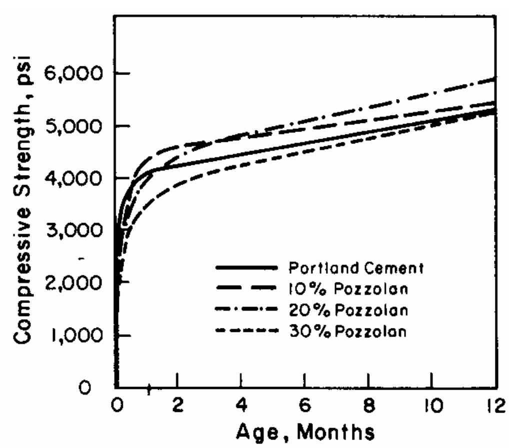

(b) Pozzolan Concrete Through 1 Year

Figure 2.4: Pozzolan Effect on Concrete Compressive Strength [Mehta 1986]

is a naturally occurring material, forms when a large amount of ground water in a volcano conduit meets with silica rich magma. Use of fly ash or slag by the FDOT is governed by function of the structure and the environmental classification. They are generally utilized in concrete for aggressive environments [FDOT 2004]. When fly ash is used, it replaces a percentage of cementitious material in the concrete mix based on FDOT requirements as follows: 18 to 50% for mass concrete, 35 ± 2% for drilled shaft concrete and 18 to 22% for all other concrete. Concrete made with different percentages of fly ash would cure at appreciably different rates. Therefore, the rate of strength gain of one fly ash concrete mix may not be used to predict the rate of strength gain of another mix.

ASTM C 989-99 classifies slag as Gr. 80, 100 or 120, based on the slag-activity index. A higher activity index generally produces a higher slag grade. Only Gr. 100 or better slag type should be used in FDOT slag concrete mixes. When slag is used, it replaces a percentage of cementitious material in the mix based on FDOT requirements as follows: 60 ± 2% for drilled shaft concrete and 25 to 70% for all other slag concretes [FDOT 2004].

2.4 Modulus of Elasticity (MOE)

Concrete does not have a truly linear region in its stress-strain curve, nor is it a truly elastic material (Fig. 2.5). Four basic types of Moduli of Elasticity (MOE) may be defined, from the plot of the stress-strain curve (Fig. 2.6):

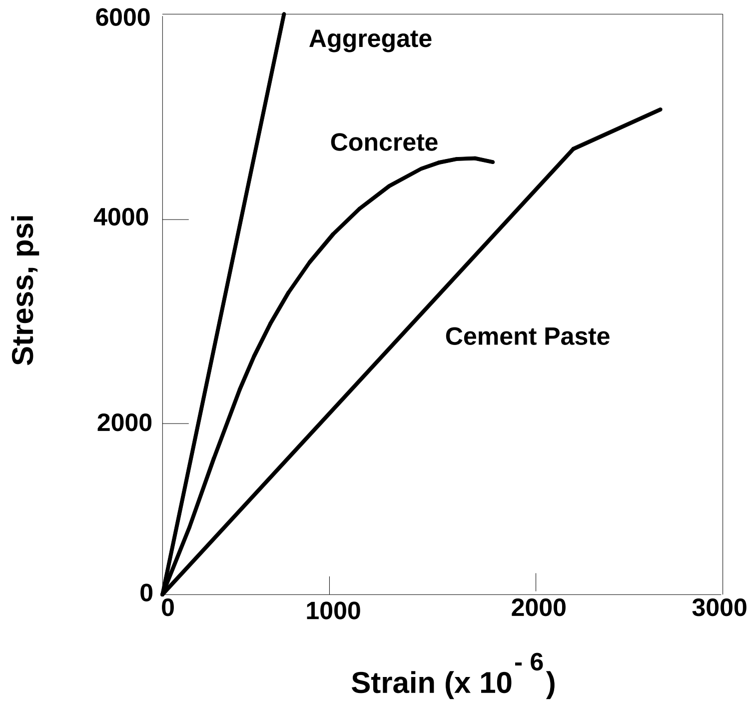

Figure 2.5: Modulus of Elasticity of Concrete, Aggregate & Cement Paste [Mehta 1986]

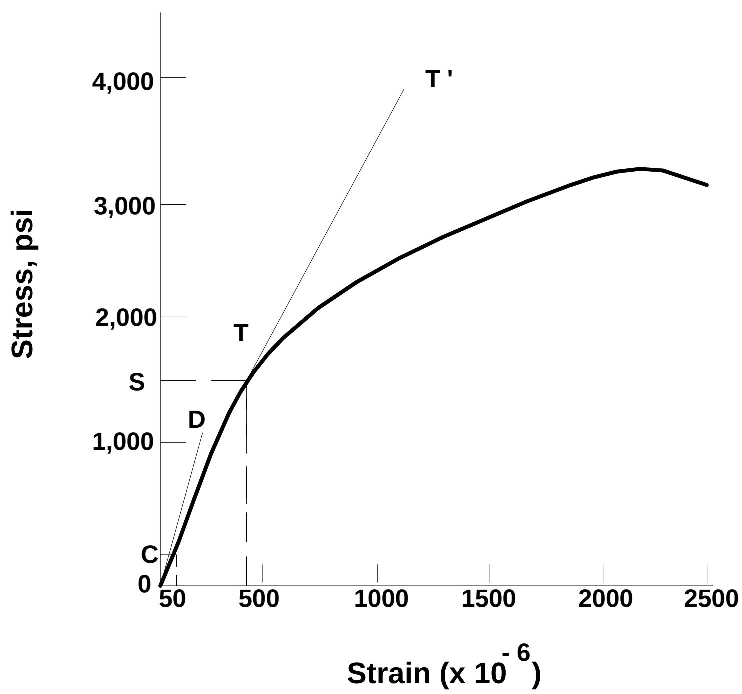

Figure 2.6: Various Elastic Moduli of Concrete [Mehta 1986]

- Tangent Modulus – This is the slope of line TT' drawn tangent to the curve at any point.
- Secant Modulus – This is the slope of the line SO drawn from the origin to the point on the curve corresponding to 40% of the ultimate strength.
- Chord Modulus – Similar to the Secant Modulus. It is the slope of the line SC drawn between the point corresponding to a strain of 50 microns and the point corresponding to 40% of the ultimate strength.
- Dynamic Modulus – This is the initial slope of the line OD from the origin and is primarily used in earthquake and impact load design [Mehta 1986].

Secant Modulus was used in this study to determine the MOE of concrete.

The most common method for determining the MOE of concrete is through empirical equations as functions of the unit weight and compressive strength of concrete. The ACI 318 MOE equation, which is valid for f'_c from approximately 400 psi to 6,000 psi and unit weights from 90 pcf to 155 pcf, is as follows [ACI 2002]:

$$E_c = 33 \cdot w^{1.5} \cdot \sqrt{f'_c} \tag{2.2}$$

where:

E_c = secant modulus of elasticity of concrete (psi)

f'_c = concrete compressive strength (psi)

w = unit weight of concrete (pcf)

Empirical equations such as Eq. 2.2 are statistically based on laboratory test results. The use of the two parameters is logical because the parameters represent various concrete characteristics of MOE. The MOE of coarse aggregate is related to its porosity, and the unit weight is a simple means of estimating the porosity of coarse aggregate. The stress-strain behavior of all three components of concrete – the aggregate, the HCP, and the transition zone – are directly influenced by their respective compressive strengths, which in turn are related to the concrete compressive strength. This means that the MOE of concrete may also be correlated to the concrete compressive strength. Slow chemical reaction between the HCP and the aggregate in the transition zone can cause a small improvement in the density and strength of the transition zone. This long-term improvement in the transition zone has a greater effect on the MOE than on the compressive strength. The use of mineral admixtures also improves the compressive strength of the transition zone similarly; however, the improvement on MOE is relatively small. Cain found a slight increase in the MOE for 90-day samples of fly ash concrete, as compared to concrete of the same compressive strength made without fly ash. However, fly ash has a much smaller effect on MOE than cement and coarse aggregate characteristics [Cain 1979, ACI 232.2R-96]. Klieger and Isberner found no considerable difference in MOE for concrete containing slag and concrete with only Portland cement [Klieger and Isberner 1967, ACI 233R-03]. Similar to mineral admixtures, the composition of the cement plays little or no role in the MOE. The degree of hydration and filling of the voids is the controlling factor affecting the MOE [ACI 225R-99].

Microcracks in the concrete transition zone increase in size and number with increased applied load. These cracks play a major role in the stress-strain behavior of the concrete member. Below about 30% of the ultimate load, the microcracks remain stable, the stress-strain curve is approximately linear, and the concrete behavior is nearly elastic. Between about 30 and 50% of the ultimate load, the microcracks increase in size and number and the material no longer behaves elastically. When the load exceeds the 30% limit and is then removed, some of the strain is recovered due to the elasticity of the individual components. However, the increased cracking in the transition zone causes a permanent strain that is not recovered. Above about 50% of the ultimate load, microcracks in the HCP begin to form and propagate [Mehta 1986]. Testing conditions also affect the MOE of concrete. Specimens that are dry tested demonstrate about a 15% lower MOE than specimens in normal wet conditions. Faster than normal loading rates increases the measured MOE by not allowing sufficient time for strain and crack propagation [Mehta 1986].

2.5 Theoretical Models

2.5.1 Current FDOT Models

The current FDOT pay reduction equations are based on a study performed by the Bureau of Reclamation approximately 25 to 30 years ago and are as follows [FDOT 2004]:

$$f'_c(28) = \frac{f_{core} \cdot 100}{F} \tag{2.3}$$

where:

$f'_c(28)$ = equivalent 28-day compressive strength

f_{core} = average core compressive strength

For Type I Cement, $F = 4.4 + 39.1. (\ln t) - 3.1. (\ln t)^2$ (2.4)

For Type II Cement, $F = - 17.8 + 46.3. (\ln t) - 3.3. (\ln t)^2$ (2.5)

For Type III Cement, $F = 48.5 + 19.4. (\ln t) - 1.4. (\ln t)^2$ (2.6)

t = number of days since concrete casting

Equations 2.3 through 2.6 determines the ratio or percentage of strength gain at a given age to the age of 28 days. It is the relative strength development as a percentage of the 28-day strength. The equivalent 28-day compressive strength is then used to determine if the FDOT specifications for the concrete compressive strength have been met. A search with the Bureau of Reclamation was performed to locate the basis and data for Eqs. 2.3 through 2.6. Personnel at the Bureau were contacted by email and telephone for assistance, and a search was conducted on the Bureau's web site. It was not possible to locate the study in their records with the limited information available, and without the approximate time-frame when the study was performed.

Section 7.1 of the FDOT Structures Design Guidelines references Eq. 5.4.2.4-1 of the AASHTO LRFD Bridge Design Specifications for prediction, and specifies that 90% of this value be used for concrete with Florida lime-rock [FDOT 2003, AASHTO 2003]. The AASHTO equation is equivalent to the ACI 318 MOE equation (Eq. 2.2). The specified 90% reduction for Florida lime-rock concrete is most likely due to consistently lower MOE values obtained, compared with FDOT concrete with other coarse aggregates. FDOT allows the use of a default unit weight of 145 pcf for concrete made with Florida lime-rock, if the unit weight is unknown. The FDOT MOE equation for Florida lime-rock concrete is as follows:

$$E_c = 30 \cdot w^{1.5} \cdot \sqrt{f'_c} \tag{2.7}$$

2.5.2 Similar Studies and Test Data

A literature search was performed to locate previous work involving similar cementitious material types for the time-dependent compressive strength portion of this study, concrete with similar coarse aggregate for the MOE portion of this study, and test data for concrete compressive strength at various ages, MOE and unit weight. No such studies pertaining to the compressive strength portion of this study were located. However, three FDOT sponsored studies were performed at the University of Florida that resulted in MOE data for concrete with Florida coarse aggregates and limited time-dependant compressive strength data for concrete with Type II cement and 20% fly ash [Amornsrivilai et al 1989, 1991, 1992].

In addition, two extensive studies performed by Jim Cook are of relevance to this study. The first study [Cook 1989] was performed at Gifford-Hill Company (HFH), Dallas, Texas, using normal weight coarse aggregates from Texas, Arizona, South Carolina and Tennessee. About 600 MOE data points were generated from this study. Aggregate size varied from 3/8 in. to 1 in, and consisted primarily of crushed limestone, granite and native gravel. The average concrete unit weight for the Texas study was 151 lb/ft^3. The second study, still ongoing at Tarmac-Florida, deals with experimental determination of MOE values for Florida Pennsuco limestone aggregate [Cook 2004]. Over 600 data points have been generated to date. The mixes used were not FDOT approved mix designs, but were proportioned so as to meet FDOT requirements for Class IV, V and VI concrete including the maximum 18% fly ash. Best fit MOE regression equations have been generated, as discussed later in this chapter.

2.5.3 Time-Dependent Compressive Strength

A search was conducted to locate existing theoretical models representing the compressive strength of concrete as a function of time. The FDOT pay reduction relationships (Eqs. 2.3 – 2.6) are functions of time in days for cement Types I, II, and III [FDOT 2004].

Compressive strength of concrete does not continue to increase indefinitely, i.e. it has a finite limit. Existing models that grow infinitely as time approaches infinity will not be considered as candidates for analysis and comparison. Measurable gain in concrete compressive strength does not occur immediately after casting. Significant setting occurs during a period of several hours, after which strength gain accelerates. A realistic plot of strength gain versus time would not go directly through the origin, but have an S-shaped inflection near the setting time. Models, which account for this offset compressive strength are preferred.

The CEB-FIP Model Code [CEB-FIP 1990, Han 1996] uses the following equation for time-dependent prediction of concrete compressive strength:

$$f_c(t) = f'_c \cdot e^{s \cdot \left[1 - \sqrt{\frac{28}{\left(\frac{t}{t_1}\right)}}\right]} \tag{2.8}$$

where:

$f_c(t)$ = compressive strength of concrete at time t

f'_c = 28-day compressive strength of concrete

t = age of concrete in days

s = variable that depends on the cement type and mineral admixture used

t_1 = 1 day

The CEB-FIP model has a finite limit and a curved setting-age offset.

The AFREM and the ACI 209 equations both use the hyperbolic model, which has a finite limit and no setting-age offset. The AFREM equation is as follows [De Larrard et al 1996]:

$$f_c(t) = \frac{t}{1.5 + 0.95 \cdot t} \cdot f'_c \tag{2.9}$$

Eq. 2.9 does not take into account the type of cement used in the concrete mix.

The ACI 209 equation has the following form:

$$f_c(t) = \frac{t}{a + b \cdot t} \cdot f'_c \tag{2.10}$$

where:

a = variable that depends on cement type and curing conditions, inverse of the initial slope

b = variable that depends on cement type and curing conditions, inverse of the ultimate strength

Eq. 2.10 with the specified values for a and b is not valid for concrete with mineral admixtures such as pozzolans and slag.

The Nykanen equation is based on the relationship for predicting the charge of a capacitor when a constant voltage is applied [Nykanen 1956, Carino and Malhotra 1991]. The equation has a finite limit and no setting age offset, and is presented in the following:

$$f_c(t) = f_{ult} \cdot \left(1 - e^{-k \cdot t}\right) \cdot f'_c \tag{2.11}$$

where:

f_{ult} = ultimate compressive strength of concrete

k = variable that depends on cement type

The model proposed by Chin [Chin 1971, Carino and Malhotra 1991] is a modified version of the hyperbolic model that accounts for the offset in setting age by forcing the plot to have a zero strength value at the determined offset age. While not an accurate model for the first few hours of curing, it is sufficiently accurate for one day age and beyond. The Chin offset-hyperbolic model has a finite limit and is as follows:

$$f_c(t) = \frac{t - t_0}{a + b \cdot \left(t - t_0\right)} \tag{2.12}$$

where:

t_0 = the offset age when setting of the concrete is assumed to start

Plowman proposed the following model for concrete compressive strength [Plowman 1956, Carino and Malhotra 1991]:

$$f_c(t) = [a + b.log(t)].f'_c \tag{2.13}$$

where:

a, b = variables related to the cement type

This model has an infinite limit, a sharp setting-age offset and is invalid for early ages.

Freiesleben and Pederson [Freiesleben and Pederson 1985, Carino and Malhotra 1991] proposed the following empirical relationship for concrete compressive strength:

$$f_c(t) = f_{ult} \cdot e^{-\left(\frac{\tau}{t}\right)^a} \cdot f'_c \tag{2.14}$$

where:

t = variable related to cement type

a = variable related to cement type (shape parameter)

Eq. 2.14 has a finite limit and a curved setting-age offset.

Lew and Reichard [Lew and Reichard 1978, Carino and Malhotra 1991] proposed the following strength-time relationship:

$$f_c(t) = \frac{f_{ult}}{1 + D \cdot log\left(t - t_0\right)^b} \cdot f'_c \tag{2.15}$$

where:

D, b = variables related to cement type

Eq. 2.15 has an infinite limit and a sharp setting-age offset.

Table 2.3 summarizes the characteristics of various concrete compressive strength models discussed herein. The ACI model (Eq. 2.10) is valid for both moist and steam curing [ACI 209R-92]. All other models are only valid for ASTM standard moist curing conditions [ASTM C 192-02].

The Lew (Eq. 2.15), Chin (Eq. 2.12), Plowman (Eq. 2.13) and the current FDOT pay reduction equations (Eq. 2.3-2.6) all incorporate a sharp setting-time offset. The CEB-FIP (Eq. 2.8) and Freiesleben (Eq. 2.14) models have the more accurate S-shaped setting-time offset where as the hyperbolic (Eq. 2.10) and Nykanen (2.11) models do not account for the setting-time offset. The Plowman, and Lew equations have infinite limits.

2.5.4 MOE Models

A literature search was performed to locate theoretical models for prediction of the concrete modulus of elasticity. The two predominant MOE relationships used are specified by ACI 318 (Eq. 2.2) and ACI 363 (Eq. 2.17). The ACI 318 MOE approach is based on a study by Pauw [Pauw 1960]. For normal weight concrete, assumed to be 150 pcf, ACI 318 specifications allow the following simplification of Eq. 2.2:

Table 2.3: Characteristics of Theoretical Concrete Compressive Strength Models

No.	Model	Limit	Setting-Time Offset	No. of Variables	Eq. No.
1	Freiesleben	Finite	S-shape	3	2.14
2	CEB-FIP	Finite	S-shape	1	2.8
3	Hyperbolic	Finite	No	2	2.10
4	Nykanen	Finite	No	2	2.11
5	Chin	Finite	Sharp	3	2.12
6	Plowman	Infinite	Sharp	2	2.13
7	Lew	Infinite	Sharp	4	2.15
8	FDOT pay reduction	N/A	Sharp	3	2.3

$$E_c = 57000 \cdot \sqrt{f'_c} \tag{2.16}$$

Although the ACI MOE equations utilize the square root of f'_c, a preliminary equation by Pauw [Pauw 1960], with the exponents optimized, yielded an exponent of 0.30 for the compressive strength, which is closer to the cube root than the square root. Previous MOE equations used by ACI 318 and ACI-ASCE 323 specifications for normal weight concrete were linear functions of the compressive strength [Pauw 1960].

ACI 363R-92 specifications contain an MOE relationship for high strength and normal weight concrete with compressive strengths ranging from 3,000 to 12,000 psi, as follows:

$$E_c = 40000 \cdot \sqrt{f'_c} + 10^6 \tag{2.17}$$

The use of the unit weight of fresh concrete and the 28-day compressive strength of concrete as MOE predictor variables has long been established through various MOE studies, and is the standard for engineering practice. Other concrete properties, such as modulus of rupture and splitting tensile strength, also use the square root of the concrete compressive strength as a predictor variable. However, research over the past few decades have shown a tendency for the MOE to be related to the cube root of the concrete compressive strength. As an example, the CEB-FIP Model Code [CEB-FIP 1990, Han 1996] specifies the following two empirical expressions to predict the dynamic modulus of elasticity.

$$E_{ci} = E_{c0} . \left(\frac{f_{cm}}{f_{cm0}} \right)^{1/3} \tag{2.18}$$

$$E_{ci}(t) = E_{ci} \cdot \sqrt{e^{s \cdot \left(1 - \sqrt{\frac{28}{\frac{t}{t_1}}}\right)}} \tag{2.19}$$

where:

E_{ci} = the tangent MOE (MPa)

E_{co} = a constant value, 2.15x10^4 MPa

f_{cm} = compressive strength of concrete at 28 days (MPa)

f_{cm0} = a constant value, 10 MPa

$E_{ci}(t)$ = time-dependent MOE (MPa)

s = a variable that depends on the cement type and mineral admixtures used

Equations 2.18 and 2.19 are independent of the unit weight of concrete. However, the variation of aggregate density is accounted for by the fact that Eq. 2.18 is valid only for quartzitic aggregates. A multiplier based on the type of coarse aggregate used is specified for Eqs. 2.18 and 2.19 in the CEB-FIP Model Code. Equation 2.18 is only valid for the 28-day compressive strength, whereas Eq. 2.19 indirectly allows for variations in compressive strength due to lower or higher ages.

The following concrete MOE equation was developed by Cook [Cook 1989] for high strength concrete.

$$E_c = w^{2.55} \cdot f'_c{}^{0.315} \qquad \text{(GFH-Texas)} \tag{2.20}$$

In Eq. 2.20, the exponent for the compressive strength is much closer to 0.33 than to 0.5. For the study performed by Cook, the concrete strength range was approximately 4,200 to 14,400 psi, and the ages ranged from seven to ninety days.

While working at Tarmac, Cook developed the following MOE equation for Florida Pennsuco limestone concrete:

$$E_c = 325{,}300.f'_c{}^{0.305} \qquad \text{(Tarmac-Florida)} \qquad (2.21)$$

As apparent from Eq. 2.21, the concrete unit weight has been eliminated as a variable in the MOE equation.

CHAPTER 3

EXPERIMENTAL SETUP

3.1 Materials

The materials used in this study were selected through consultation with FDOT personnel to be representative of the material types typically used in FDOT concrete. The materials are cement, mineral admixtures, chemical admixtures, and coarse and fine aggregates.

Types I, II, and III portland cements were utilized in this study, because current FDOT pay reduction equations differ according to cement types. Two types of mineral admixtures were used, a Class F fly ash and a Grade 100 slag. The FDOT State Materials Office performed a chemical and physical analysis on samples of the cement, fly ash, and slag used in this study. The analysis results are shown in Tables 3.1 through 3.3. Some information not reported by the FDOT was obtained from the manufacturers.

The chemical admixtures used were a Type A water reducer and an air entrainer. Three different coarse aggregates were used in this study, representative of the common aggregates used in FDOT concrete, as follows:

Table 3.1: Chemical and Physical Analysis of Cement

Parameter	Cement Type		
	I	II	III
Chemical Analysis			
Silicon Dioxide (SiO_2), %	20.91	20.45	19.14
Aluminum Oxide (Al_2O_3), %	4.08	5.60	5.54
Ferric Oxide (Fe_2O_3), %	4.01	4.33	3.85
Calcium Oxide (CaO), %	64.28	63.97	63.58
Magnesium Oxide (MgO), %	2.01	0.78	1.04
Sulfur Trioxide (SO_3), %	2.59	2.81	4.05
Alkalis as Na_2O equivalent, %	0.54	0.60	0.59
Insoluble Residue, %	0.13	0.19	0.30
Loss on Ignition, %	1.4	1.3	2.6
Dicalcium Silicate (C_2S), %	13.28	18.80	10.60
Tricalcium Silicate (C_3S), %	62.29	53.19	59.10
Tricalcium Aluminate (C_3A), %	4.02	7.50	8.17
Tetracalcium Aluminoferrite (C_4AF), %	12.19	13.18	11.72
Physical Analysis			
Blaine Fineness, m^2/kg	397	385	*562
Blaine Fineness, ft^2/lbm	1938	1880	*2744
Autoclave Expansion (Soundness), %	+0.03	+0.03	+0.01
Gilmore Setting Time – Initial, min	159	140	142
Gilmore Setting Time – Final, min	205	202	275
Compressive Strength - 3 days, psi	3310	3610	3020
Compressive Strength - 7 days, psi	4280	4810	4760

*Fineness for the Type III cement supplied by the manufacturer.

Table 3.2: Chemical and Physical Analysis of Fly Ash

Parameter	Value	ASTM C 618 Class F Specifications
Chemical Analysis		
Sum of SiO_2, Al_2O_3, & Fe_2O_3, %	88.0	min 70.0
Sulfur Trioxide (SO_3), %	0.5	max 5.0
Moisture Content, %	0.2	max 3.0
Loss on Ignition, %	3.4	max 6.0
Alkalis as Na_2O equivalent, %	1.89	max 1.5
Calcium Oxide (CaO), %	4.54	N/A
Physical Analysis		
Fineness, amount retained on No. 325 sieve, %	24	max 34
Stength Activity Index - 7 days, %	77	min 75
Strength Activity Index - 28 days, %	---	min 75
Water Requirement, %	100	max 105
Autoclave Expansion (Soundness), %	-0.01	max 0.8
Specific Gravity	2.08	N/A

Note: Uniformity requirements not tested due to single sample analyzed.

Table 3.3: Chemical and Physical Analysis of Slag

Parameter	Value	ASTM C 989 Grade 100 Specifications
Chemical Analysis		
Sulfide Sulfer (S), %	0.8	max 2.5
Sulfate ion reported as SO_3, %	1.9	max 4.0
Physical Analysis		
Fineness, amount retained on No. 325 sieve, %	13	max 20
Air Content, %	---	max 12
Slag Activity Index - 7 days, %	85	min 70
Slag Activity Index - 28 days, %	116	min 90
Specific Gravity	*2.92	N/A

*Specific Gravity supplied by the manufacturer.

Table 3.4: Aggregate Characteristics

Aggregate	Grade or Fineness Modulus	Bulk Specific Gravity (SSD)	Absorption (%)	Source	Pit #
Coarse Aggregate					
Brooksville	# 57	2.43	3.98	Brooksville, FL	08-005
River Gravel	# 67	2.63	0.60	Chattahoochee, FL	50-120
Calera	# 57	2.72	0.37	Calera, AL	AL 149
Fine Aggregate					
Sand	2.36	2.63	0.50	Quincy, FL	50-382

- Brooksville lime rock from Brooksville, FL,
- River gravel from Chattahoochee, FL,
- Calera lime rock from Calera, AL.

The fine aggregate used is a natural silica sand from Quincy, FL. Characteristics of the three coarse aggregates and the fine aggregate are presented in Table 3.4.

3.2 Design Mix

FDOT state materials office personnel assisted in selecting a single base Class IV concrete design mix from FDOT's design mix database. The design mix selected is a hot weather fly ash mix, FDOT Mix Number 07-0004, issued on April 4, 1990, and is presented in Table A.1 in the appendix. Instead of investigating a separate slag concrete mix, the base fly ash mix was modified for the replacement of the fly ash with slag. The 80% to 20% cement to fly ash ratio was replaced with a 50% to 50% cement to slag ratio. Several factors were considered in selection of a popular and representative mix. A mix with Florida lime rock was chosen because it is the most frequently used aggregate in FDOT concrete. The mix contains a relatively low percentage of Air Entraining Admixture (AEA), minimizing variations in air content. Type II cement used in the base mix is the most common cement type used in FDOT concrete. A mix with the most commonly used admixtures was desired so as to be representative of a typical FDOT Class IV concrete.

According to FDOT Specifications [FDOT 2004], the fresh concrete must be held at a minimum temperature of 94° F for 90 minutes after the initial mixing is completed. The drum is to be turned for 30 seconds every five minutes and for one minute at the end of the 90-minute initial mixing. Problems with performing the hot weather mixing procedure during cold weather months was encountered in a recent FDOT study [Jin and Yazdani 2001]. The heating of the mix for the specified duration caused excessive water and slump loss, making the mix difficult to use, and in some cases completely unusable. The hot weather concrete mixing for the current study would be performed during the cold weather months of January through April. To alleviate the problem, with permission from FDOT personnel, a normal mixing procedure was followed herein. To account for this change, the Type D admixture (retarder/water-reducer) was reduced by 33%, making it equivalent to a Type A admixture (water-reducer only).

3.3 Test Matrices

Both the compressive strength test and MOE tests were performed with the fly ash mix, in which the cement type and aggregate type were substituted. Only the compressive strength test was performed with the modified slag mix. In the all slag mixes, the Brooksville aggregate was used with substitution of cement types. The test matrices for the various material substitutions yielded nine fly ash mixes and three slag mixes, as shown in Tables 3.5 and 3.6, respectively. The ages for the strength tests were 1, 7, 28, 60, 90, 180 and 365 days, whereas the ages for the MOE tests were 1, 7, 28, 90 and 365 days.

Table 3.5: Fly Ash Test Matrix

Concrete Mix ID	Cement Type	Aggregate Type
1FC	I	Calera
1FB	I	Brooksville
1FG	I	River gravel
2FC	II	Calera
2FB	II	Brooksville
2FG	II	River gravel
3FC	III	Calera
3FB	III	Brooksville
3FG	III	River gravel

No. of Cylinders for Each Mix Combination for f'_c Testing

7 ages [1, 7, 28, 60, 90, 180 & 365days]

3 cylinders for each test age

21 cylinders for each mix combination

Total no. of cylinders for 9 concrete mixes = 9 x 21 = 189
Total no. of compressive strength data points for 9 concrete mixes = 189 ÷ 3 = 63

No. of Cylinders for Each Mix Combination for MOE Testing

5 Ages [1, 7, 28, 90 & 365 days]

2 Cylinders for each data point

10 Cylinders for each mix combination

Total no. of cylinders for 9 concrete mixes = 9 x 10 = 90
Total no. of MOE data points for 9 concrete mixes = 90 ÷ 2 = 45

Total no. of cylinders for 9 Mix Combinations = *189 + 90 = 279*

Table 3.6: Slag Test Matrix (f'_c Test Only)

Concrete Mix ID	Cement Type	Aggregate Type
1SB	I	Brooksville
2SB	II	Brooksville
3SB	III	Brooksville

No. of Cylinders for Each Mix Combination
7 ages [1, 7, 28, 60, 90, 180 & 365days] 3 cylinders for each test age
21 cylinders for each mix combination

Total no. of cylinders for 3 concrete mixes = 3 x 21 = 63

3.4 Mixing, Casting and Curing

Mixing and curing of the concrete batches were accomplished using ASTM specifications [ASTM C 192-02]. The absorption and moisture content of the aggregates were determined so they could be accounted for in the water added in the mix. Based on advice from FDOT personnel, quantities of coarse and fine aggregates were adjusted to account for changes in materials used in the base design mix, while the weight of total cementitious material was held constant. Differences in specific gravity of the aggregates were used to adjust their weights so that the volumetric ratios of the aggregates for the original one cubic yard design mix could be maintained. Some of the cements and pozzolans used had different specific gravities than those specified in the base design mix. This caused a change in the volume of the cubic yard mix. Since the weights of the cementitious materials must remain the same, the mix was adjusted by using more or less coarse and fine aggregate. The volumetric ratio of coarse to fine aggregate was held constant in this adjustment. The weight of the coarse and fine aggregates were changed to maintain a one cubic yard design mix, while also maintaining the weights of cement, pozzolan and water. The small quantity of water in the admixtures was not considered to be a part of the mixing water. The final mix proportions are shown in Table A.2 in the Appendix.

Though all mixes were variations of the Class IV base mix, the w/c ratios of the individual mixes were varied from the design mix in order to achieve variations in the concrete mix. The w/c ratio for the 12 batches ranged from 0.35 to 0.51, with an average value of 0.41. This average value is the specified w/c ratio of the base design mix. Changes in the w/c ratio primarily affect the compressive strength, providing a range of data points and validity to the results. Variations in the w/c ratio and compressive strength were accounted for in the compressive strength data values through normalizing, as described in Section 4.4. Variations in the compressive strength and unit weight of the MOE data sets were accounted for in the regression analysis with the actual strength and unit weight values.

The w/c ratio variations are statistically beneficial. The concrete unit weight varied due to the substitution of coarse aggregates and cementitious materials with different specific gravities. Further variability in the unit weight due to the alteration of the w/c ratio helped ensure a wide range of values for regression analysis, as well as improving the applicability of the developed models to a sufficiently broad range of concrete unit weights. Variations in w/c ratio also improved the range of concrete compressive strengths that would be usable with the developed MOE equations.

Substitution of the materials may have caused some of the plastic concrete properties to vary from those specified in the base design mix. Limited variations from these parameters should not adversely affect the outcome of the results of the study. Consistency in these properties between the different concrete batches is not required for either the compressive strength or the MOE portions of the study.

3.4.1 Absorption and Moisture Content

Absorption is the amount of water retained within the pores of the coarse and fine aggregate after saturation and removal of the excess surface moisture. Absorption and specific gravity values [ASTM C 127-01, ASTM C 128-01e1] for the fine and coarse aggregates were obtained from the suppliers. The aggregates were maintained in a saturated condition and the moisture content of the aggregates were determined regularly before casting [ASTM C 566-97]. The aggregate absorption was subtracted from the moisture content to yield the surface moisture, which was counted as part of the mixing water for the design mix. The actual weights of the wet aggregates and water used were determined as follows:

$$W'_a = W_{ssd} \cdot (1 + M_s) \tag{3.1}$$

$$W'_w = W_w - W_{ssd} \cdot Ms \tag{3.2}$$

where:

W'_a = weight of aggregate to weigh out (adjusted for surface moisture), lb

W_{ssd} = saturated-surface-dry weight of aggregates for mix, lb

W'_w = weight of water to weigh out (adjusted for aggregate moisture), lb

W_w = weight of total water in mix, lb

M_s = surface moisture of aggregate (moisture minus absorption), %

3.4.2 Concrete Mixing

Concrete mixing was performed using a 6 ft^3 Gilson HM-224 electric mixer according to ASTM C 192 specifications (Fig. 3.1). The Type A admixture was added to a portion of the mixing water and the AEA was added to a separate portion of the mixing water. The two admixtures were not mixed together. The coarse aggregate, Type A admixture, and part of the water were added to the mixer prior to starting the mixer. The mixer was started and the remaining ingredients were added in the following order. The

Figure 3.1: Concrete Mixing

Figure 3.2: Concrete Casting & Slump Test

fine aggregate was added, followed by the cement and pozzolan. The remaining water and AEA were added last. The mixer was kept rotating throughout the process. After all ingredients were added, the concrete was mixed for three minutes, followed by a three-minute rest and another two-minute mixing period. The concrete was covered while not being mixed, and during most periods of mixing as well.

3.4.3 Concrete Casting

The 6 by 12 in. test cylinders were cast according to ASTM C 192-02 procedure (Fig. 3.2). The concrete was placed in a damp mixing pan immediately after mixing was complete. The cylinder molds were placed on a hard, flat and level surface, and concrete was placed in the cylinder molds in three equal layers. Each layer was rodded 25 times, the bottom layer throughout its depth, and the top two layers 1 in. beyond the bottom of the layer. After each layer was rodded, the cylinder was hand tapped 10 to 15 times to release any trapped air. Excess concrete was struck off with the tamping rod and the surface was troweled smooth. Finally, plastic lids were placed on the cylinder molds to maintain their shape and prevent loss of water by evaporation.

3.4.4 Concrete Curing

The concrete specimens were cured in accordance with ASTM C 192-02 specifications. The cylinder molds were placed inside a temperature-controlled laboratory on a flat, hard and level surface, free of movement or vibration (Fig. 3.3). The specimens were removed from the molds 24 ± 8 hr after casting. The tops of the specimens were ground smooth using a masonry rubbing stone to help facilitate even pressure distribution during compressive strength and MOE testing. The concrete cylinders were then placed

Figure 3.3: Cast Concrete in Cylinder Molds

Figure 3.4: Curing Tank with Heater and Thermometer

in water curing tanks approximately 8 ft x 2 ft x 2 ft in size. The water tanks were maintained at 73 ± 3 °F for the entire curing process by means of curing tank heaters. The temperature of the tanks was monitored regularly (Fig. 3.4).

3.5 Plastic Property Testing of Fresh Concrete

Immediately after mixing of the concrete and placing a portion in the damp mixing pan, the plastic properties of the fresh concrete were determined, concurrent with the casting of the cylinders. The following tests were performed: slump, temperature, air content, and unit weight. The slump of fresh concrete was measured according to ASTM C 143-03 specifications (Fig. 3.2). During the slump test, the temperature of the concrete was measured according to ASTM C 1064-03.

The air content of the fresh concrete was measured using the volumetric method in accordance with ASTM C 173-01e1 specifications (Fig. 3.5). The unit weight of the concrete was measured according to ASTM C 138-01a specifications using a ½ ft^3 metal container (Fig. 3.6).

3.6 Testing of Hardened Concrete

The time of casting and testing of each cylinder was recorded in order to keep track of the exact age of each cylinder. The MOE cylinder pairs and the corresponding three compressive strength cylinders were tested concurrently. ASTM C 39-03 specifications provides age tolerances for concrete strength testing from ages 24 hr to 90 days. However, to provide slight flexibility in test scheduling and to improve accuracy,

Figure 3.5: Volumetric Air Content Test

Figure 3.6: Unit Weight Test

the exact ages of the specimens were determined for each strength and MOE test. The age for each cylinder was determined individually, and the average age of the three strength cylinders and the two MOE cylinders were found separately..

3.6.1 Compressive Strength Test

The compressive strength test was performed in accordance with ASTM C 39-03 specifications (Figs. 3.7 and 3.8). The capping used was unbonded neoprene pads, as specified in ASTM C 1231-00e1 standards. Specimens were tested in the moist condition shortly after being removed from the curing tank. A Forney compression machine using a load rate of 20 to 50 psi/s was used. Each cylinder was brought to complete failure and the maximum load recorded. For each cylinder, the maximum load was divided by its area to determine the compressive strength. The average strength of the three cylinders for each batch and age combination was recorded as the final compressive strength.

3.6.2 Modulus of Elasticity Testing

The MOE test immediately followed the compressive strength testing. The test was performed according to ASTM C 469-02 specifications. Two modifications were made to the ASTM C 469-02 procedure. The ASTM standard states that one cylinder is to be tested two consecutive times, and the average used at the MOE. However, as requested by FDOT personnel, the procedure was modified by testing two different cylinders once each, and averaging the results. A compressometer with a dial gage was centered on and attached to the specimen to be tested (Fig. 3.9). The neoprene pads and retainers were placed on the cylinder, and the specimen was placed in the Forney

Figure 3.7: Cylinder Test in Forney Compression Machine

Figure 3.8: Three Cylinders from Strength Test and Two Cylinders from MOE Test

Figure 3.9: Compressometer Attached to MOE Test Sample

compression machine. The test was performed by loading the specimen at a rate of 35 ± 5 psi/s, until the load applied was at least 40% of the compressive strength of the specimen. The compressive strength was previously determined, prior to of the MOE testing. The ASTM standard also states that multiple loadings up to 40% of f'_c are to be applied with no data recorded for the first load. The specimen is then to be unloaded at the 35 ± 5 psi/s rate. This pre-load is needed to seat the gages and make sure there are no problems before performing the test.

Manually reading the compressometer dial gage at the exact load of 40% of f'_c would have been difficult. Therefore, multiple readings were taken and linear interpolation used to determine the stress and strain for the 40% of f'_c level. Most of the MOE cylinders were brought to imminent failure with strain/force pairs measured throughout the test. Approximately six to twelve readings of the dial and force display were taken for each cylinder to ensure a good stress-strain curve and an accurate slope line.

CHAPTER 4

RESULTS AND ANALYSIS OF TIME DEPENDENT COMPRESSIVE STRENGTH DATA

4.1 Mix Designation

Each of the 12 test concrete batches were designated a three-character identifier, as shown in Tables 3.5 and 3.6. The first number signifies the cement type, whereby Types I, II and III cement mixes are represented by numbers 1, 2 and 3, respectively. Letters ‘F’ and ‘S’ in the second character are used to represent fly ash or slag mix, respectively. In the third character, letters ‘B’, ‘G’ and ‘C’ are used to designate Brooksville lime rock, river gravel and Calera lime rock, respectively. An example mix designation is 3FG, which contains Type III cement, fly ash and river gravel.

4.2 Plastic Property Results

The plastic test properties of the 12 concrete batches are presented in Table 4.1. The properties reported are slump, air content, unit weight and temperature. Most of the slump and air content results fell within the acceptance range for the base design mix. All three slag mixes demonstrated slightly greater slump than that specified in the acceptance limit. One slag mix also contained air content greater than the limit. Temperature for all

Table 4.1: Plastic Test Properties and Classification for Test Mixes

Batch ID*	Slump (in)	Air Content (%)	Unit Weight (pcf)	Temp. (°F)	28-Day f'_c (psi)	w/c Ratio	FDOT Class Excluding Slump Requirement
1FB	4.25	3.75	142	63.5	5,190	0.42	III
2FB	3.25	4.25	142	59.0	5,630	0.41	IV
3FB	4.25	3	141	72.5	5,420	0.43	III
1FG	5.25	5.5	143	58.0	4,730	0.38	II (Bridge Deck)
2FG	4.25	3	146	66.0	5,380	0.35	III
3FG	4.25	2.75	147	83.0	4,720	0.39	II (Bridge Deck)
1FC	5.5	4.75	145	84.0	5,200	0.51	III
2FC	2.25	5.25	149	65.0	6,300	0.41	V (Special)
3FC	3.25	2.75	150	81.5	5,320	0.40	III
1SB	7	8.5	135	69.5	4,830	0.43	None
2SB	5.5	4	143	51.0	6,180	0.42	V (Special)
3SB	6	3.25	143	51.5	6,580	0.40	V

*Batch ID:

1st character: cement (Types I, II and III)
2nd character: mineral admixture (F: fly ash, S: slag)
3rd character: aggregate (B: Brooksville, G: river gravel, C: Calera)

mixes were below that specified in the base mix design, and most unit weights were slightly greater. Casting outside during cold weather resulted in the wet concrete temperature to be lower than the hot weather mix specifications. As discussed in Section 3.4, it was expected that substitution of various components would essentially make the mix different than the base mix. As a result, some of the plastic property values were expected to be different than that specified in the base mix. Mixes 2FB and 2FC most closely represent the base Class IV mix with Type II cement, fly ash and Florida limerock coarse aggregate. Table 4.1 shows that the plastic properties from both these mixes conform to the base mix specifications. These variations resulted in broader types of concrete mixes being investigated, increasing the scope of the analysis.

4.3 Compressive Strength Results

The compressive strength test results for all batches are presented in Table 4.2. The batch ID in this table only shows the last two letters of the identifier, which represent the mineral admixture and aggregate type. The designation of cement type is shown as a column heading. The 28-day compressive strengths of the batches ranged from 4,721 psi to 6,576 psi, with an average of 5,546 psi. Mixes 2FB and 2FC mixes that represent the base Class IV mix used, reached the target 28-day compressive strength of 5,500 psi. Because of the ingredient substitution, the variation in the compressive strength is expected, and this beneficial variation helps to make the developed models applicable to various mixes with a broad range of compressive strengths. Table 4.1 shows the FDOT classification [FDOT 2004] of the 12 concrete batches used in this study.

Table 4.2: Compressive Strength Test Results

Batch ID*	Target Age (day)	Cement Type					
		I		II		III	
		Age (day)	f'_c (psi)	Age (day)	f'_c (psi)	Age (day)	f'_c (psi)
FB	1	1.12	2,009	1.00	859	0.99	2,809
	7	7.00	3,671	7.23	4,496	6.93	4,488
	28	28.08	5,192	28.33	5,631	27.86	5,422
	60	60.00	6,010	59.98	6,111	59.73	6,089
	90	89.94	6,009	90.62	6,320	92.06	6,464
	180	181.00	6,684	186.64	6,605	179.94	6,843
	365	367.88	6,862	373.72	6,442	375.83	6,637
FG	1	1.03	1,400	1.01	1,478	1.00	2,360
	7	7.31	3,216	6.85	3,721	7.04	4,066
	28	28.15	4,734	28.20	5,378	28.10	4,721
	60	60.18	5,262	60.09	5,705	61.02	5,318
	90	90.14	5,852	89.79	6,533	90.81	5,804
	180	181.92	6,520	179.95	6,863	182.81	6,232
	365	365.26	6,905	368.07	7,267	364.86	6,878
FC	1	1.00	2,012	1.02	1,873	0.99	3,260
	7	7.21	3,769	7.15	4,927	7.00	4,670
	28	28.87	5,197	29.24	6,299	27.94	5,322
	60	60.92	6,100	59.78	7,388	60.98	6,362
	90	88.86	6,545	89.87	7,543	89.95	6,747
	180	180.70	7,149	180.07	7,899	179.87	7,559
	365	364.98	7,664	364.83	8,432	365.02	7,455
SB	1	1.03	669	0.99	446	1.01	1,399
	7	7.36	2,324	7.04	3,374	7.05	4,884
	28	28.36	4,825	28.24	6,177	27.99	6,576
	60	60.31	5,483	60.27	7,418	60.91	7,259
	90	90.07	5,761	92.20	7,493	89.10	7,449
	180	179.95	5,871	180.99	7,693	180.94	7,710
	365	373.04	5,947	368.07	8,097	365.02	7,508

*Batch ID:

1st character: mineral admixture (F: fly ash, S: slag)

2nd character: aggregate (B: Brooksville, G: river gravel, C: Calera)

4.4 Analysis of Fly Ash Mix Data

The fly ash and slag mix strength data were initially analyzed separately. The two data sets were compared after the analysis to determine if the data sets should be merged.

4.4.1 Normalization of Data

The procedure to determine time-dependent models to represent concrete compressive strength was based on regression analysis using specific mathematical models. The time-dependent strength data for each batch ranging from 1 day to 365 days yielded 7 age-strength data pairs, as seen in Table 4.2. The fly ash mixes yielded 9 cement type and aggregate data combinations for each age. As described in Ch. 3, the actual ages of the cylinders at the time of testing were determined for the regression analysis, and the target ages are mentioned herein for discussion only. As a first step, the 9 fly ash data sets were normalized by dividing each strength data by the 28-day compressive strength. This made each data value a convenient unitless ratio, and will hereafter be refereed to as the "strength-ratio". The normalized data value corresponding to 28 day age was exactly unity. The purpose of the normalization was two fold. Firstly, all three aggregate data sets for a particular cement type could be combined into a single data set, with resulting 18 age-strength data pairs. The data sets could not be combined in the raw absolute strength form because the material substitutions yielded different design strengths, and were not directly comparable. Secondly, the developed strength models must be in the strength-ratio form so that they could be used for various concrete classes with different strengths.

4.4.2 Candidate Strength Model Selection

The minimum criterion required for the candidate models is a finite strength limit as the concrete age approaches infinity. This will conform to the fact that concrete compressive strength never exceeds a certain maximum threshold as the concrete ages. Other preferences include an 'S' shaped setting-time offset and an optimum number of regression variables in the models. Too few variables may make the models inaccurate, while too many variables may make them complex and hard to use. Table 2.3 shows the seven selected models with these characteristics. The Freiesleben and CEB-FIP models have an 'S" shaped setting-time offset and a finite strength limit as the concrete age approaches infinity. Therefore, these two models were selected herein as candidates. The Hyperbolic strength model has a finite strength limit and only two regression variables. Although this model does not account for the setting-time offset, this model is specified by ACI 209R-92, and was, therefore, selected herein as a candidate. The Nykanen model was also chosen as a candidate because it has a finite limit and only two regression variables. The Chin model was not considered herein because it is similar in form to the Hyperbolic model.

The four selected candidate strength models, the Freiesleben, CEB-FIP, Hyperbolic, and Nykanen are shown as items 1-4 in Table 2.3.

4.4.3 Combination of Data Sets

FDOT specification Section 346 allows the substitution of coarse aggregate of the same type from a different source in an approved concrete mix when the aggregate to be substituted is also from an approved source and has similar physical and chemical properties. Therefore, the next step was to combine the three aggregate strength-ratio data sets for a particular cement type to form one single set of 18 data pairs. Regression analysis using the first candidate model (described in Section 4.4.2) was then performed on the combined set. The developed strength-ratio model did not yield a value of unity at 28 days. The combined cement type data set was then divided by the predicted strength-ratio at 28 days, and the regression analysis was repeated with the new re-normalized data set. After this second regression analysis, the iterated model produced a unit strength-ratio at 28 days, as needed. This iterative regression process was then repeated for data from mixes with the other two cement types. The whole process was repeated for the other candidate strength models. After all candidate strength-ratio models were developed for the three cement types, their ability to accurately represent the data was compared to find the best fitting models.

4.4.4 Measures of Model Accuracy

The Coefficient of Determination, commonly referred to as the R^2 value, is the most common test statistic used to determine the quality of fit for a linear regression model to a set of data points. This test statistic is not valid for non-linear relationships such as the strength-age relationship of concrete [Bates 1988, Myers 1986, Wetherill 1986]. Therefore, a different adequacy indicator was used herein to quantify the quality of the regression fit. The test statistic chosen herein was the Standard Error of Estimate [Triola 1998]:

$$S_e = \sqrt{\frac{\Sigma \; (y - y')^2}{n - 2}} \tag{4.1}$$

where:

S_e = standard error of estimate

y = observed values of the compressive strengths for a particular cement type

y' = predicted values of the compressive strength

n = number of data points

The Coefficient of Determination is an absolute assessment of the quality of regression fit. The R^2 values will always be between 0 and 1, and the quality of a single model fit may be assessed through the proximity of the R^2 value to unity (the perfect fit). Conversely, the Standard Error of Estimate, hereafter represented by the term "error" in this report, is a relative assessment of the quality of regression fit. This tool is useful in comparing the regression fit of various models, thereby identifying the best fit model with the smallest error. The error test statistic only reveals which model has the best fit, and does not provide an absolute quantified value representing the quality of fit.

Residuals are defined as the differences between the actual compressive strength-ratio data and the predicted values. They show a linear interpretation of how well the predicted values fit the data. Residual plots for a good fitting regression model will appear evenly and randomly dispersed about the zero axis.

4.4.5 Results of Regression Analysis

Regression analysis was performed on the fly ash strength-ratio data sets using the four candidate models. The error was calculated for each strength-ratio model and the results of the three best models were plotted. The Nykanen model demonstrated a significantly higher error than the other three models. Therefore, this model was only applied to the data with Type II cement. The regression models were in the form of the normalized strength-ratio data. The 28-day compressive strength [$f'_c(28)$] was inserted on the right hand side of all regression equations presented herein to express the absolute time-dependent compressive strength. The equations for fly ash concrete compressive strengths are presented below:

Freiesleben Models:

Cement Type I: $$f_c(t) = 2.04 \cdot e^{-\left(\frac{8.31}{t}\right)^{0.276}} . f'_c(28) \tag{4.2}$$

Cement Type II: $$f_c(t) = 1.37 \cdot e^{-\left(\frac{2.89}{t}\right)^{0.514}} . f'_c(28) \tag{4.3}$$

Cement Type III: $$f_c(t) = 2.07 \cdot e^{-\left(\frac{5.38}{t}\right)^{0.191}} . f'_c(28) \tag{4.4}$$

CEB-FIP Models:

Cement Type I: $$f_c(t) = e^{0.344 \cdot \left(1 - \sqrt{\frac{28}{t}}\right)} . f'_c(28) \tag{4.5}$$

Cement Type II: $$f_c(t) = e^{0.324 \cdot \left(1 - \sqrt{\frac{28}{t}}\right)} . f'_c(28) \tag{4.6}$$

Cement Type III: $$f_c(t) = e^{0.203 \cdot \left(1 - \sqrt{\frac{28}{t}}\right)} \cdot f'_c(28) \qquad (4.7)$$

Hyperbolic Models:

Cement Type I: $$f_c(t) = \frac{t}{5.18 + 0.815 \cdot t} \cdot f'_c(28) \qquad (4.8)$$

Cement Type II: $$f_c(t) = \frac{t}{4.15 + 0.852 \cdot t} \cdot f'_c(28) \qquad (4.9)$$

Cement Type III: $$f_c(t) = \frac{t}{1.85 + 0.934 \cdot t} \cdot f'_c(28) \qquad (4.10)$$

Nykanen Model:

Cement Type III: $$f_c(t) = 1 \cdot \left(1 - e^{-0.341 \cdot t}\right) \cdot f'_c(28) \qquad (4.11)$$

The FDOT pay reduction models were also fitted to the cement type data sets for comparison purposes. The errors for the four candidates models and the FDOT pay reduction equations are presented in Table 4.3. It may be observed that the Freiesleben model has the lowest error for cement types I and III data, while the CEB-FIP model performed best for type II cement data. The overall average errors show that the Freiesleben model is the best fit to all fly ash strength-ratio data among the models chosen. The Nykanen model for Type III cement data had significantly greater error than the other models. The FDOT pay reduction models demonstrated significantly greater errors than all candidate models for each cement type category. The average error for the

Table 4.3: Standard Error of Estimates for Candidate Fly Ash Strength-Ratio Models (x 10^{-3})

Cement Type	Candidate Models				
	Freiesleben	**CEB-FIP**	**Hyperbolic**	**Nykanen**	**FDOT Pay Reduction**
I	43.1	67.3	92.6	-	146.3
II	65.5	48.1	58.0	-	203.7
III	53.0	73.5	104.2	213.4	113.3
Average	**53.9**	**63.0**	**84.9**	**-**	**154.4**

FDOT pay reduction models is almost three times that of the average error for the Freiesleben model.

The plots of the developed strength-ratio Freiesleben models for various cement types and fly ash data are shown in Figs. 4.1 through 4.3. Figure 4.2 additionally displays the plot of time-dependent strength-ratio data for concrete with Type II cement and with 20% fly ash, from the 1989 University of Florida study [Amornsrivilai et al 1989]. Figure 4.4 summarizes the plots from Figs. 4.1 – 4.3 with the three aggregate data pairs at each age averaged for clarity of presentation. The residuals plotted against age for the Freiesleben models are shown in Figs. 4.5 through 4.7. Figures 4.8 - 4.10 show the plots of the developed CEB-FIP, Hyperbolic strength-ratio models, and the existing FDOT pay reduction model, respectively. The average strength-ratio data for each cement type are also plotted in these figures.

4.4.6 Assessment of Results and Comparison of Fly Ash Strength-Ratio Models

Visual inspection of the plots and inspection of Table 4.3 reveal that the Freiesleben strength-ratio model is the best fit for fly ash data with Types I and III cement. Figures 4.2 and 4.8 show that the Freiesleben and CEB-FIP models are similar in their quality of fit for the Type II cement data. This similarity is supported by Table 4.3, which shows that the CEB-FIP model error for the Type II cement data is slightly lower than that for the Freiesleben model.

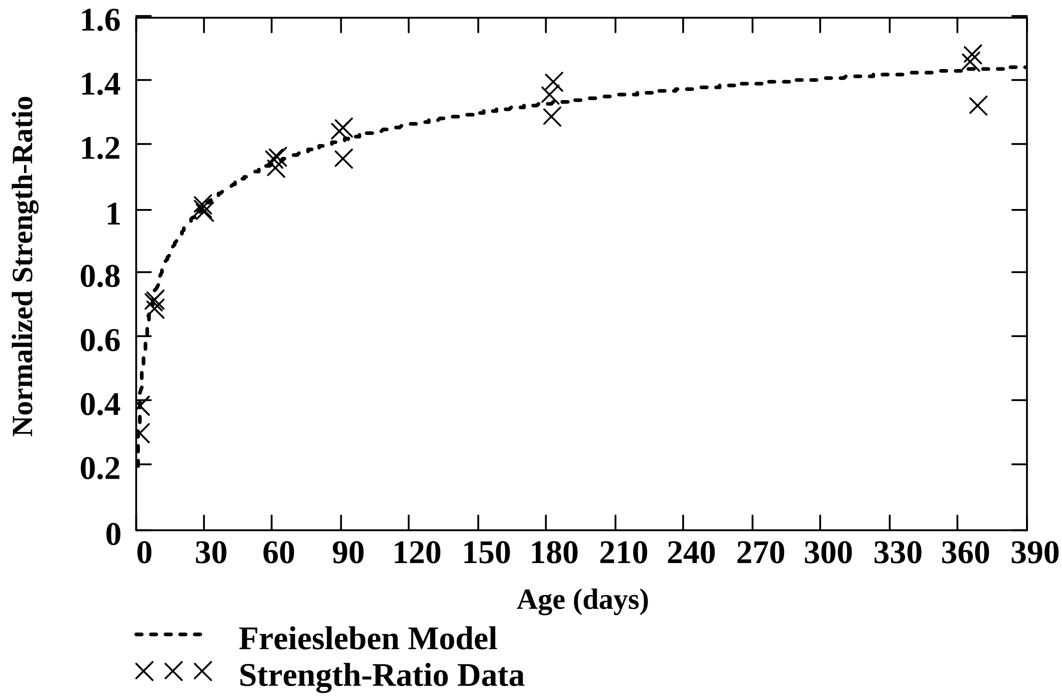

Figure 4.1: Strength-Ratio Freiesleben Model for Fly Ash and Type I Cement Mix Data

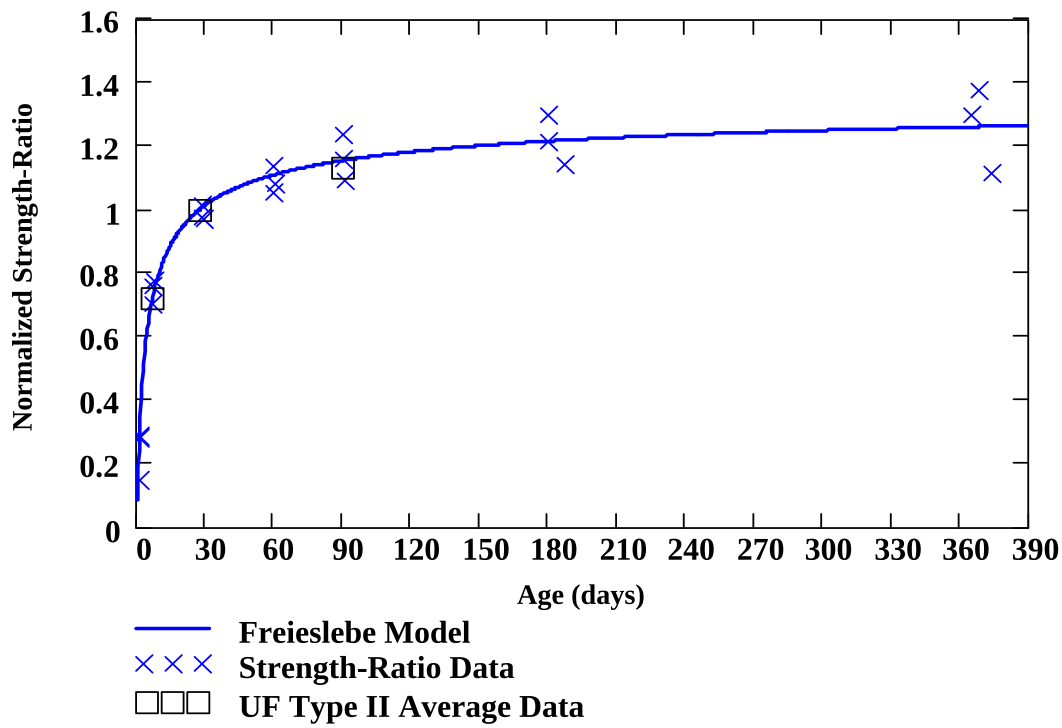

Figure 4.2: Strength-Ratio Freiesleben Model for Fly Ash and Type II Cement Mix Data [Amornsrivilai et al 1989]

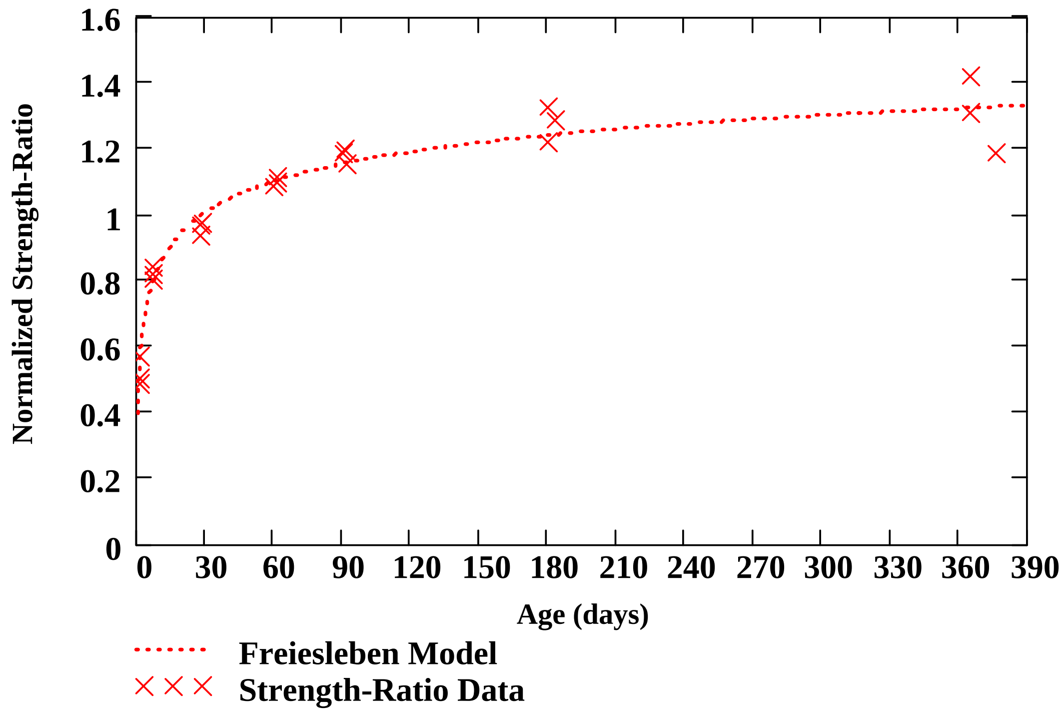

Figure 4.3: Strength-Ratio Freiesleben Model for Fly Ash and Type III Cement Mix Data

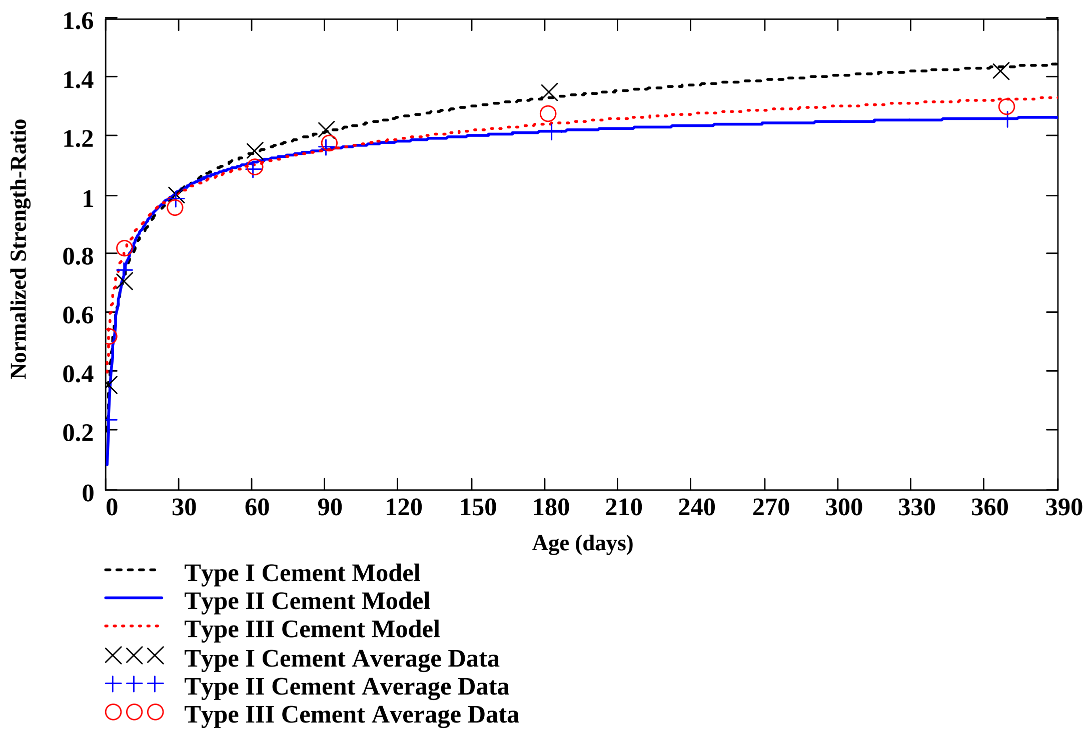

Figure 4.4: Strength-Ratio Freiesleben Model for Various Cement Types, Fly Ash Data

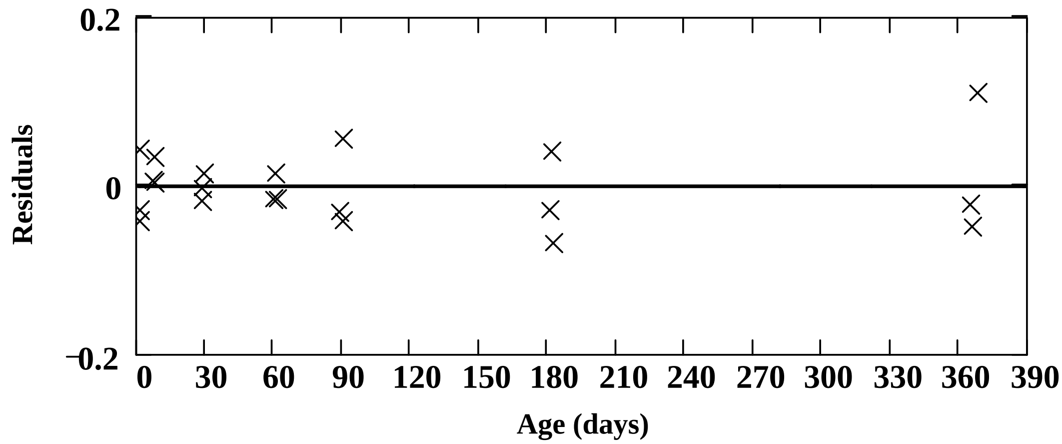

Figure 4.5: Residuals for Freiesleben Fly Ash Type I Cement Strength-Ratio Model

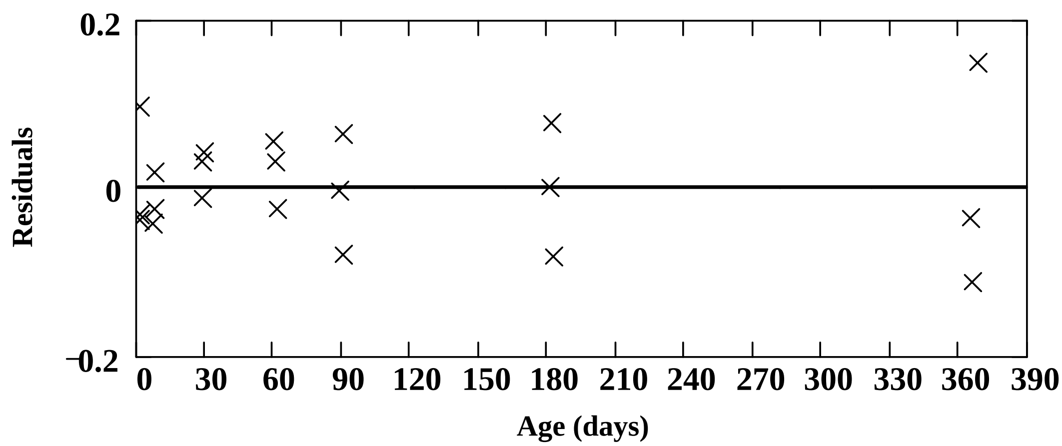

Figure 4.6: Residuals for Freiesleben Fly Ash Type II Cement Strength-Ratio Model

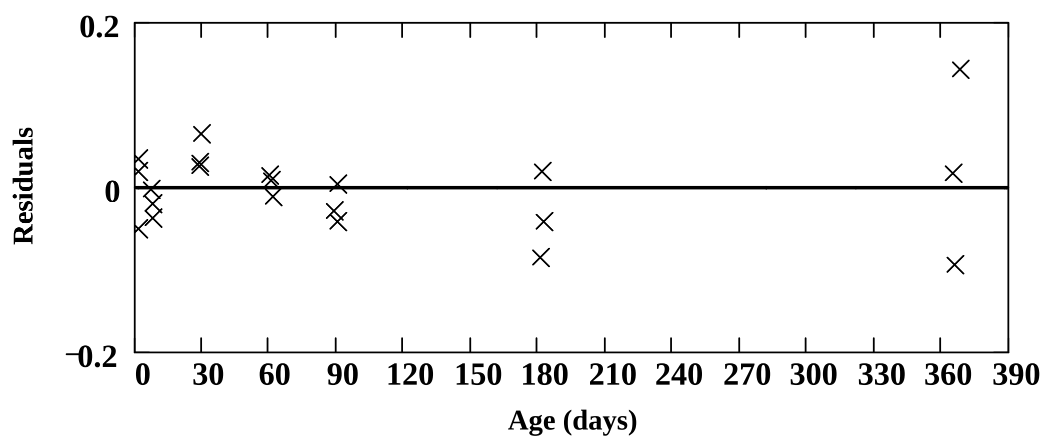

Figure 4.7: Residuals for Freiesleben Fly Ash Type III Cement Strength-Ratio Model

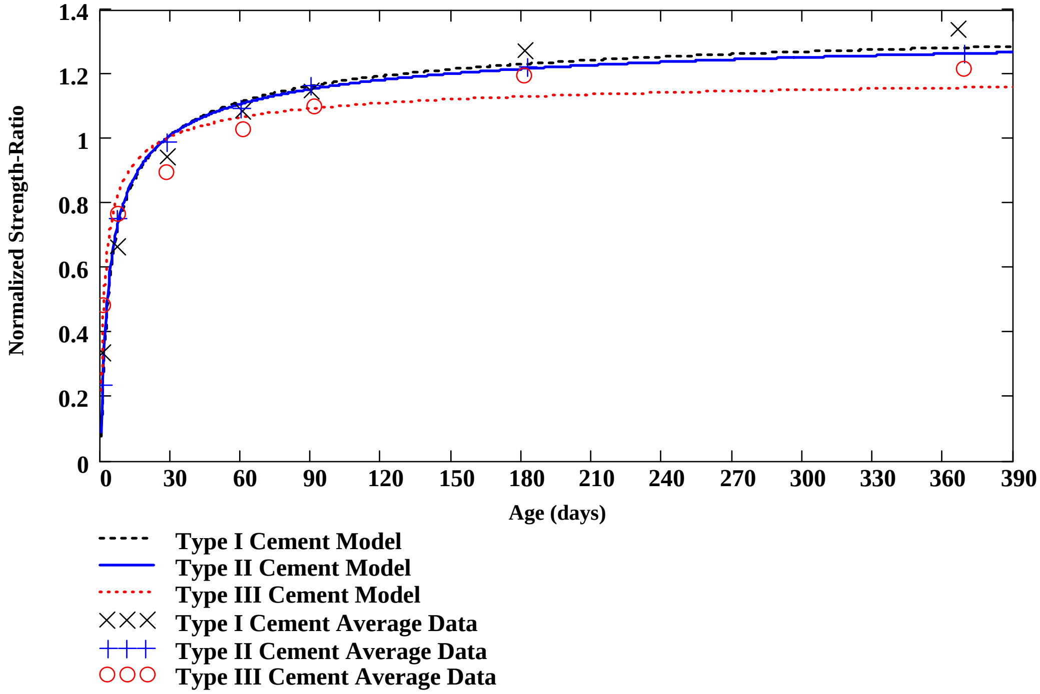

Figure 4.8: Strength-Ratio CEB-FIP Models for Various Cement Types, Fly Ash Data

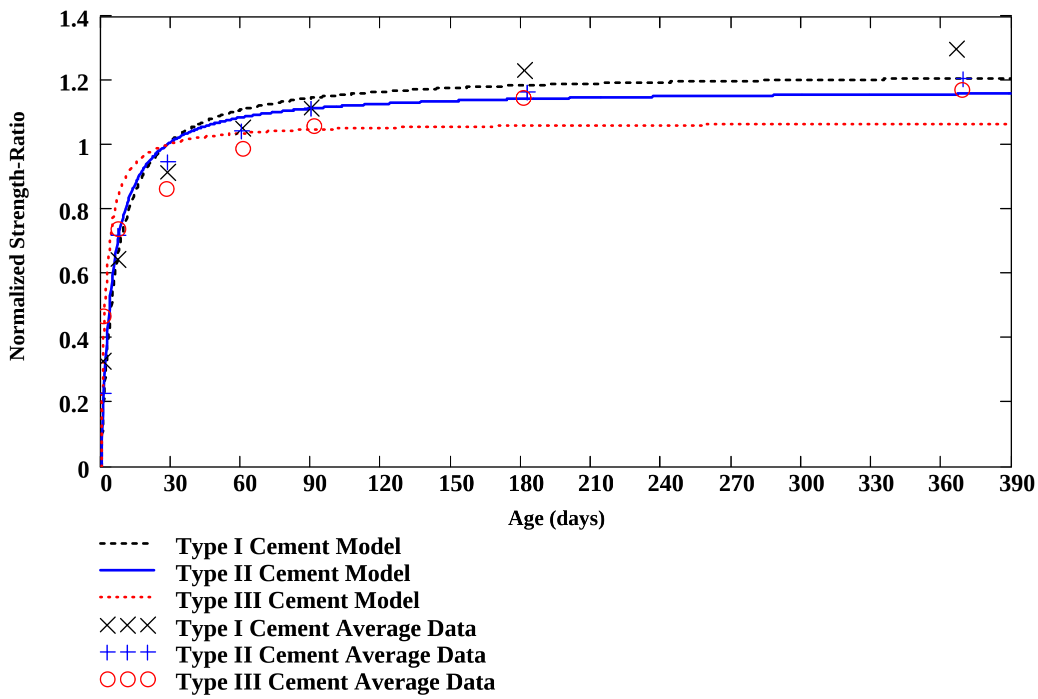

Figure 4.9: Strength-Ratio Hyperbolic Model for Various Cement Types, Fly Ash Data

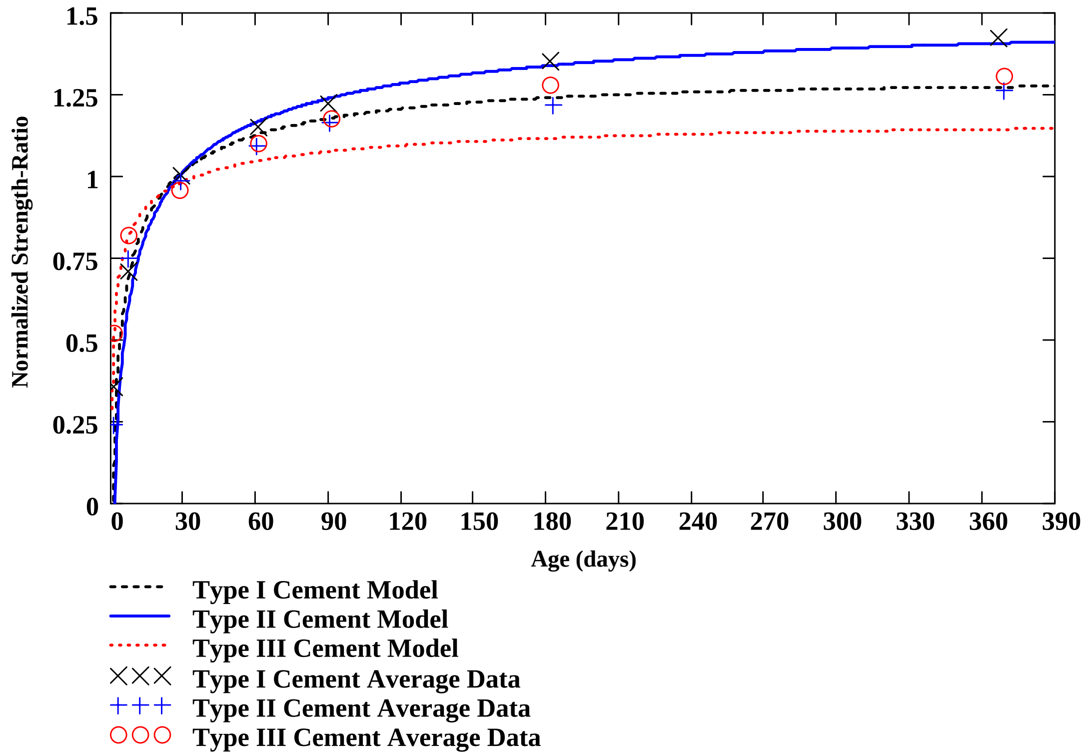

Figure 4.10: Strength-Ratio FDOT Pay Reduction Model for Various Cement Types, Fly Ash Data

The plotted strength-ratio data for the fly ash concrete with the three cement types do not follow established trends for non-pozzolan concrete. Based on industry experience, known theory about concrete curing, and current models such as ACI 209R-92 (Eq. 2.10), faster curing cements generally yield lower ultimate strengths for mixes without fly ash. Such concrete with Type III cement demonstrate the highest strength-ratio during the first few days of curing. The strength for such Type II cement concrete would be the lowest. Strength-ratios after 28 days tend to be lowest for the non-pozzolanic Type III cement batches, and highest for Type II batches. Figure 4.4 shows that the data from this study is consistent with this trend before 28 days. However, the data trend is different beyond 28 days. The strength-ratio data for concrete with Type I cement is greater than that for Type III cement mixes. However, the data for Type II cement mixes is smaller than both Type I and III cement mix data. This is most likely due to a difference in curing behavior for pozzolan mixes as compared to non-pozzolan mixes. The UF Type II cement data shown in Fig. 4.2 is the average of seven different batches that were individually normalized using their respective 28-day compressive strengths [Amornsrivilai et al 1989]. The visual inspection of this data supports the validity of the data for the Type II cement batches obtained in the current study. Prior to about one month age, Class F fly ash does not contribute significantly to the strength of the concrete (Fig. 2.4). Since this contribution is delayed, the strength gain for the first few weeks of curing for concrete with all cement types is similar to concrete batches made without pozzolan.

The Freiesleben model has a better ability to accurately account for the second phase of curing brought on by the fly ash at around one month age. This flexibility is important and beneficial in accurately reflecting the curing rates of concrete with fly ash. The Freiesleben models have acceptable residual plots with good dispersions about the zero axis. The equations are not overly complex, nor do they have a large number of independent variables. Based on these findings and comparison to the other candidate models, the Freiesleben model is the best choice to represent the strength-ratio data for fly ash concrete. Although the CEB-FIP model is a better fit to the Type II cement batch data, only one strength-ratio model for all cement batches is desirable for simplicity.

Figure 4.10 shows the FDOT pay reduction equations plotted with the normalized data. This graphical comparison along with the large standard error of estimate presented in Table 4.3 shows the inadequacy of the FDOT equations to accurately represent the strength variation of Types I, II and III cement concrete with fly ash.

4.5 Analysis of Slag Mix Data

4.5.1 Candidate Model Selection and Regression Analysis

The procedure for regression analysis of strength-ratio data from the slag batches was basically the same as that followed for the fly ash batches. Because only one aggregate type was used in the slag batches, there was no need to merge various aggregate based data sets. The three best candidate models identified for the fly ash batches were chosen as the candidate models for the slag mixes.

4.5.2 Results of Analysis

The strength-ratio regression equations for the three slag concrete candidate models are as follows:

Freiesleben Models:

Cement Type I: $$f_c(t) = 1.26 \cdot e^{-\left(\frac{7.06}{t}\right)^{1.06}} . f'_c(28) \tag{4.12}$$

Cement Type II: $$f_c(t) = 1.37 \cdot e^{-\left(\frac{6.02}{t}\right)^{0.747}} . f'_c(28) \tag{4.13}$$

Cement Type III: $$f_c(t) = 1.21 \cdot e^{-\left(\frac{2.36}{t}\right)^{0.672}} . f'_c(28) \tag{4.14}$$

CEB-FIP Models:

Cement Type I: $$f_c(t) = e^{0.485 \cdot \left(1 - \sqrt{\frac{28}{t}}\right)} . f'_c(28) \tag{4.15}$$

Cement Type II: $$f_c(t) = e^{0.490 \cdot \left(1 - \sqrt{\frac{28}{t}}\right)} . f'_c(28) \tag{4.16}$$

Cement Type III: $$f_c(t) = e^{0.305 \cdot \left(1 - \sqrt{\frac{28}{t}}\right)} . f'_c(28) \tag{4.17}$$

Hyperbolic Models:

Cement Type I: $$f_c(t) = \frac{t}{7.61 + 0.728 \cdot t} \cdot f'_c(28) \tag{4.18}$$

Cement Type II: $$f_c(t) = \frac{t}{7.48 + 0.733 \cdot t} \cdot f'_c(28) \tag{4.19}$$

Cement Type III: $$f_c(t) = \frac{t}{3.74 + 0.866 \cdot t} \cdot f'_c(28) \tag{4.20}$$

The calculated errors for the three models and the FDOT pay reduction equations are presented in Table 4.4. The average errors show that the Hyperbolic model has the best overall fit to the slag batches strength-ratio data, with the Freiesleben model being a close second. The average error for the FDOT pay reduction equations was almost four times that of the average error for the Hyperbolic model.

Figures 4.11 through 4.13 are plots of the developed Freiesleben strength-ratio models for slag mixes with Types I, II and III cement, respectively. Figure 4.14 is a combination data plot for all three slag-cement data sets together with the Freiesleben models. Figures 4.15 and 4.16 show combination data plots for the three cement types data together with the developed CEB-FIP and Hyperbolic models, respectively.

4.5.3 Assessment of Results and Comparison of Slag Strength-Ratio Models

The slag strength-ratio data adhere more closely to typical expected trends for concrete made without mineral admixtures than the fly ash data trends observed earlier. This may be explained by the differences between the curing rates of slag and fly ash

Table 4.4: Standard Error of Estimates for Candidate Slag Strength-Ratio Models (x 10^{-3})

Cement Type	Candidate Models			
	Freiesleben	Hyperbolic	CEB-FIP	FDOT Pay Reduction
I	62.4	43.9	82.1	106.8
II	33.2	33.5	61.3	134.1
III	21.6	18.3	46.8	133.2
Average	**39.1**	**31.9**	**63.4**	**124.7**

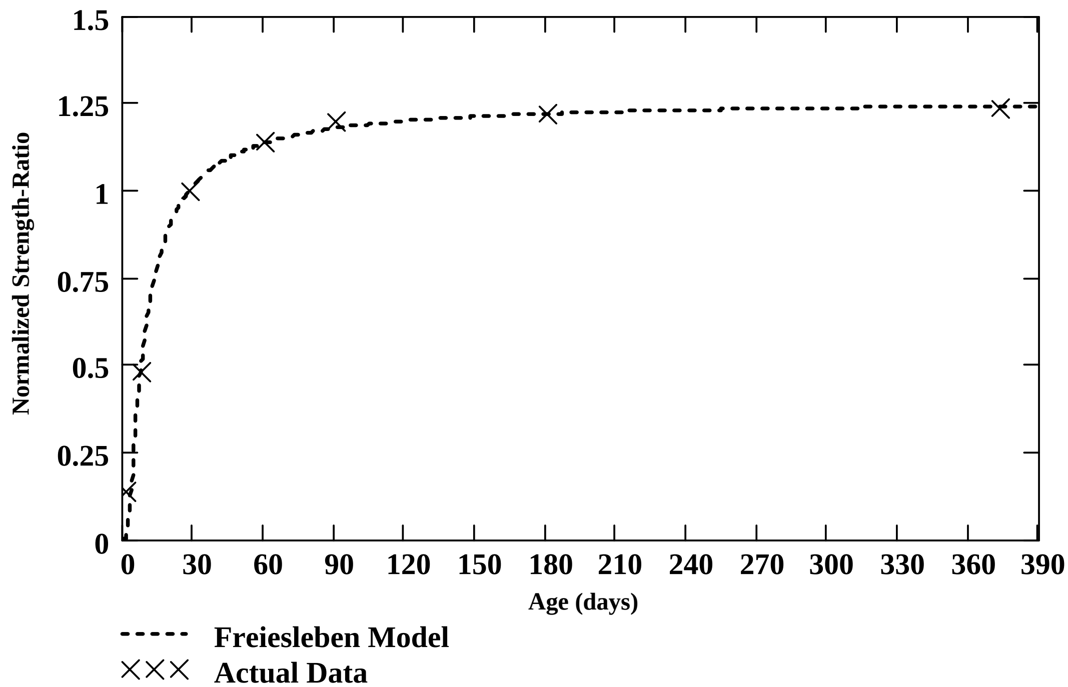

Figure 4.11: Strength-Ratio Freiesleben Model for Slag and Type I Cement Mix Data

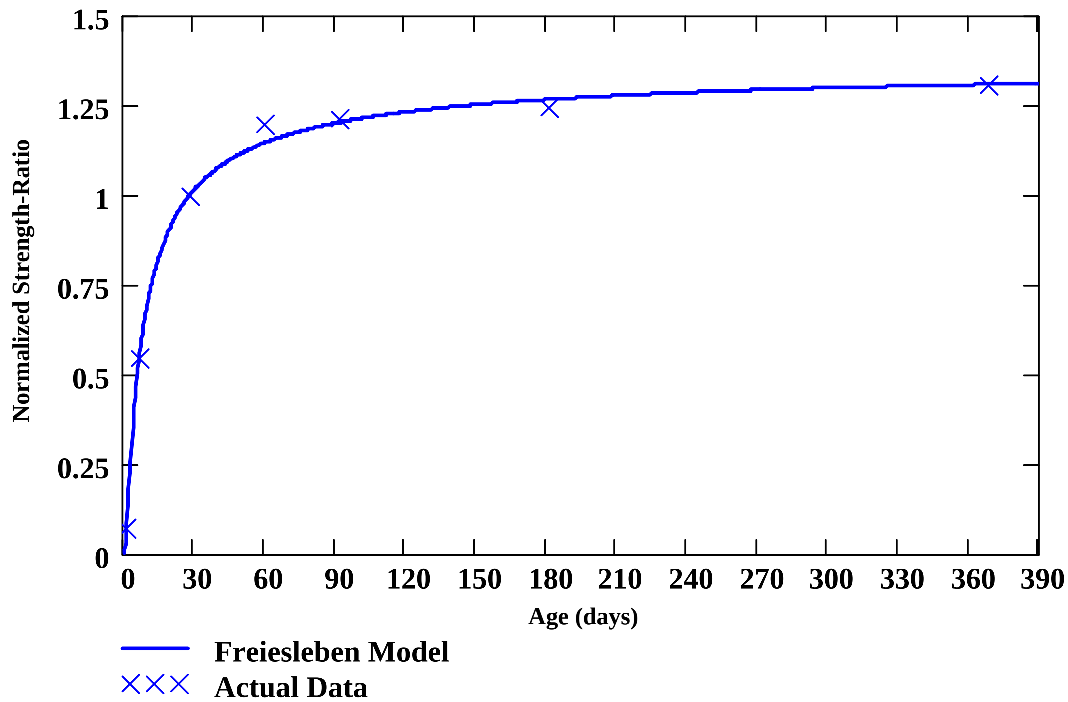

Figure 4.12: Strength-Ratio Freiesleben Model for Slag and Type II Cement Mix Data

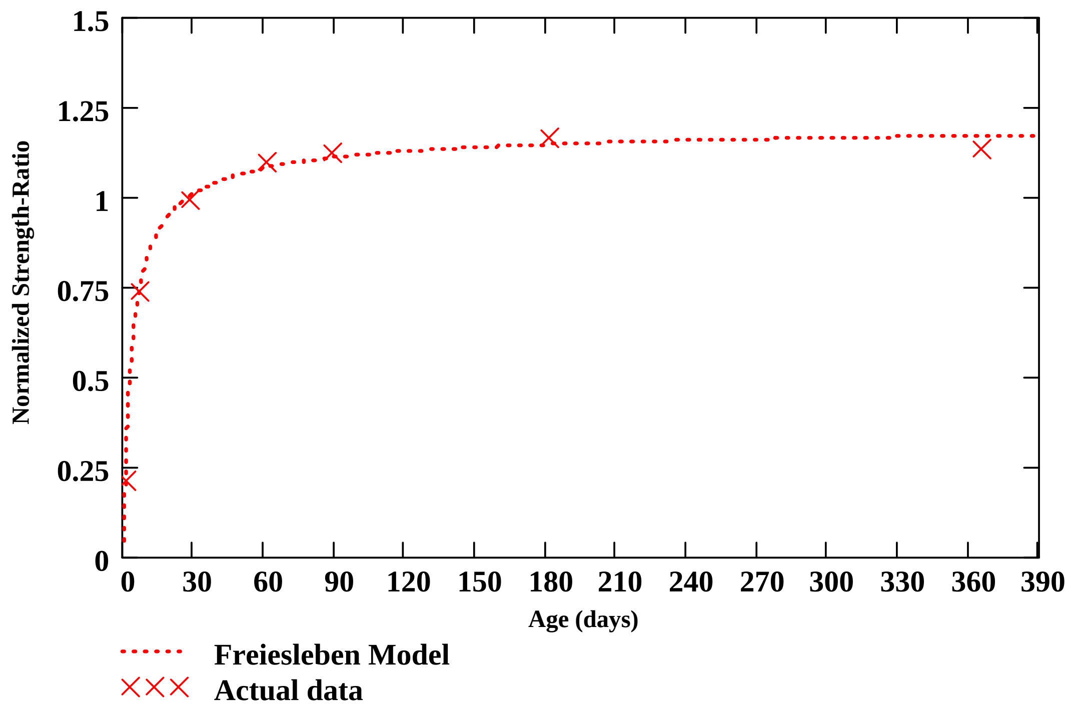

Figure 4.13: Strength-Ratio Freiesleben Model for Slag and Type III Cement Mix Data

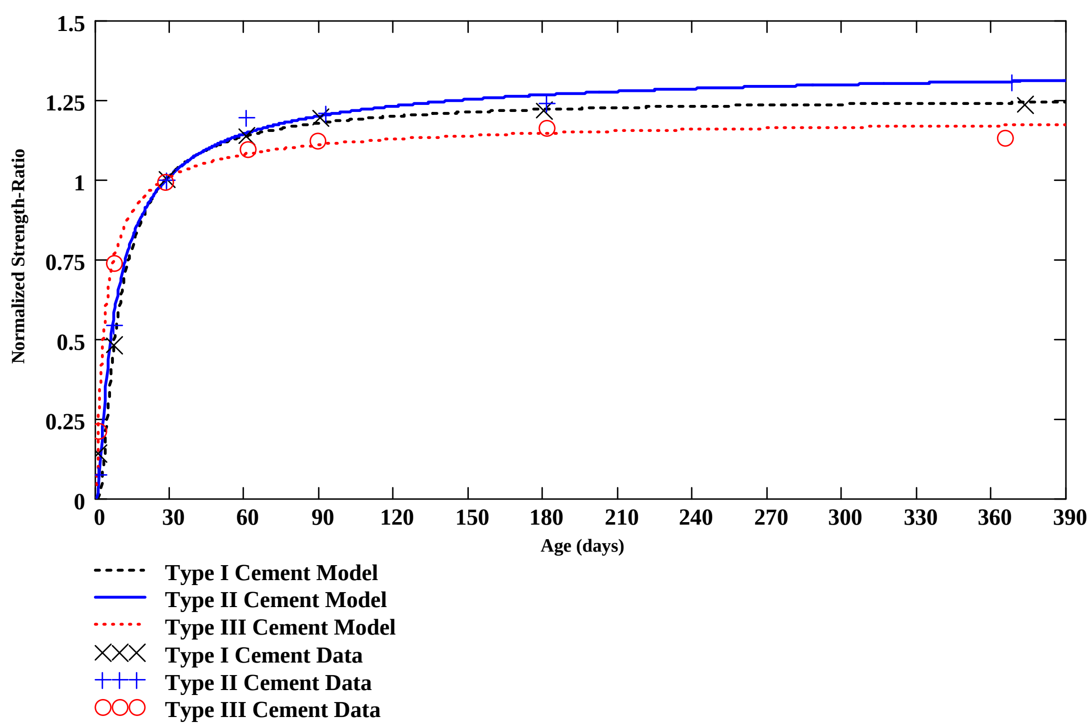

Figure 4.14: Strength-Ratio Freiesleben Model for Various Cement Types, Slag Data

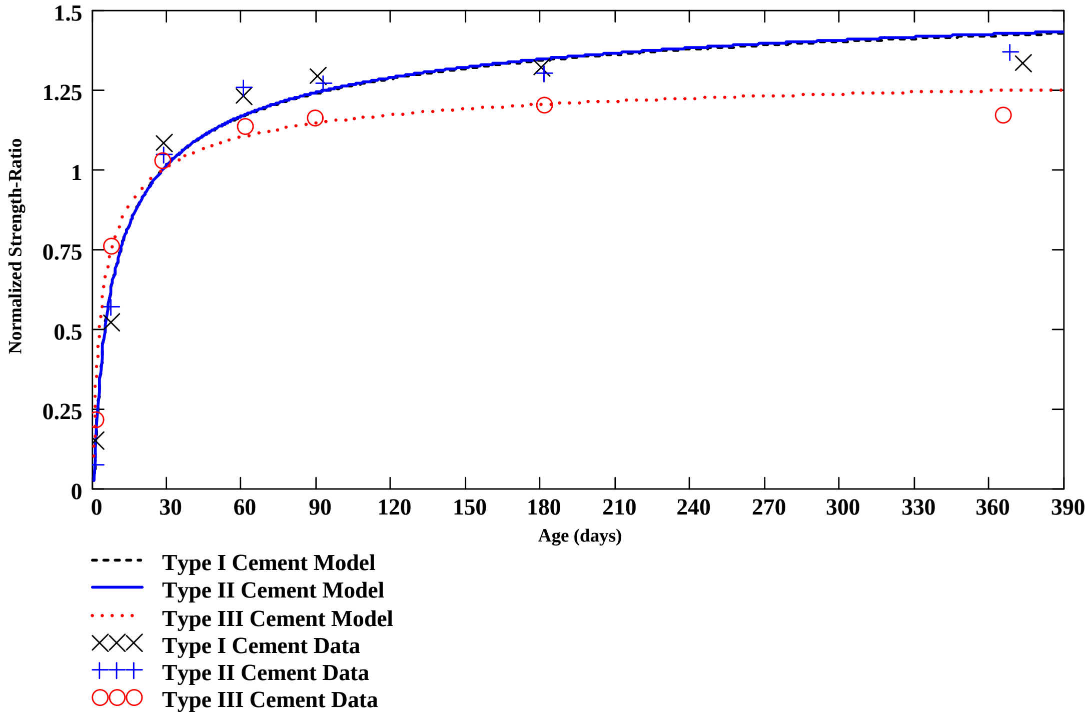

Figure 4.15: Strength-Ratio CEB-FIP Model for Various Cement Types, Slag Data

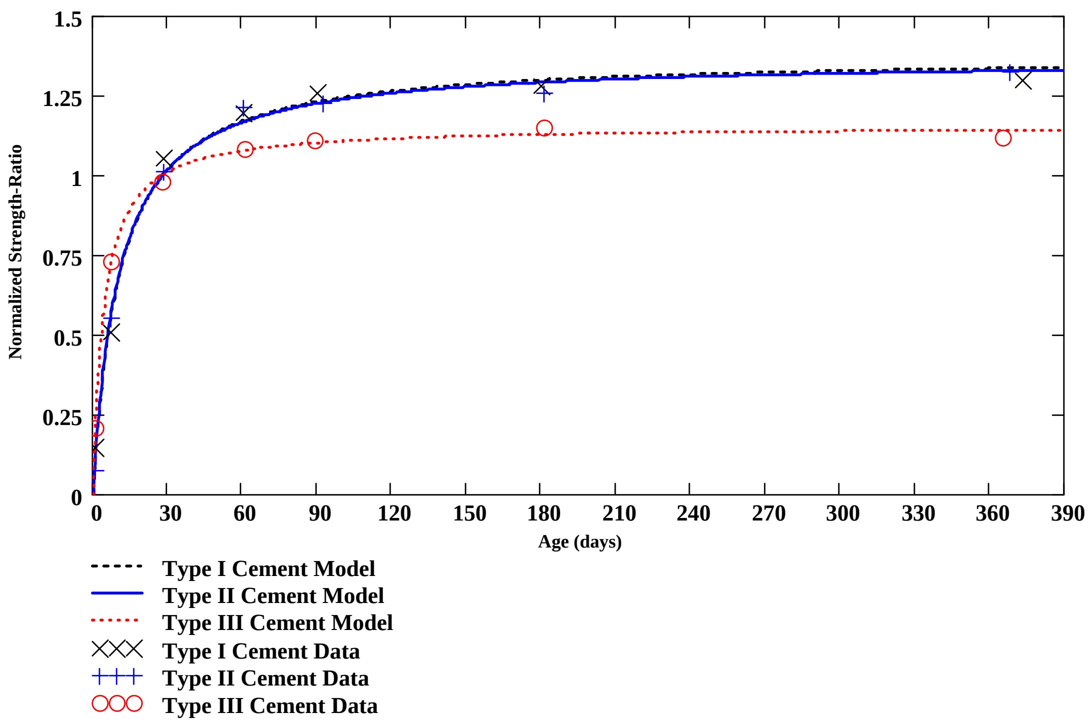

Figure 4.16: Strength-Ratio Hyperbolic Model for Various Cement Types, Slag Data

concrete. The contribution of the pozzolanic fly ash to concrete strength is not apparent until after one month age. The cementitious slag starts contributing to the strength of concrete usually within seven days of casting (Fig. 2.3) [Mehta 1986]. This means that the strength contribution of slag to the concrete strength is similar to that of the cement in the slag batches.

Comparison of the plots of the Freiesleben and Hyperbolic strength-ratio models confirms the errors reported in Table 4.4. The CEB-FIP models resulted in the highest average error of the three candidate models, and it is observed in Fig. 4.15 that the models do not fit the data very well. Both the Freiesleben and the Hyperbolic Models are observed to fit the actual strength-ratio data well, as evidenced from the errors in Table 4.4. Although the Hyperbolic strength-ratio model for slag concrete has the smallest error, both models have very close average errors. Therefore, to maintain consistency with the models chosen for fly ash concrete, the Freiesleben model was also chosen herein to represent the strength-ratio of slag concrete. Table A.3 in the appendix shows the compressive strengths normalized using the respective Freiesleben model 28-day predicted values for each cement type.

4.5.4 Comparison of Fly Ash and Slag Models

The developed strength-ratio candidate models for the fly ash and slag mixes must be compared to judge the appropriateness of merging the two sets of data and the resulting regression models. Figures 4.17 through 4.19 are combination strength-ratio plots from the Freiesleben fly ash and slag models with the FDOT pay reduction equations plotted simultaneously for comparison.

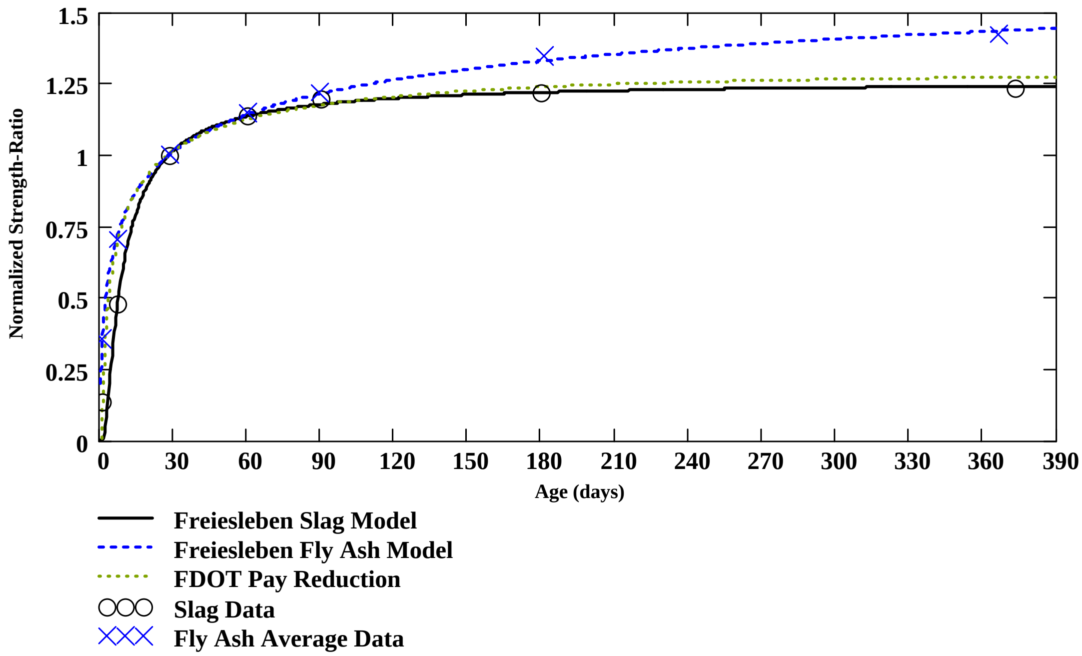

Figure 4.17: Comparison of Freiesleben Fly Ash and Slag Models for Type I Cement Mixes

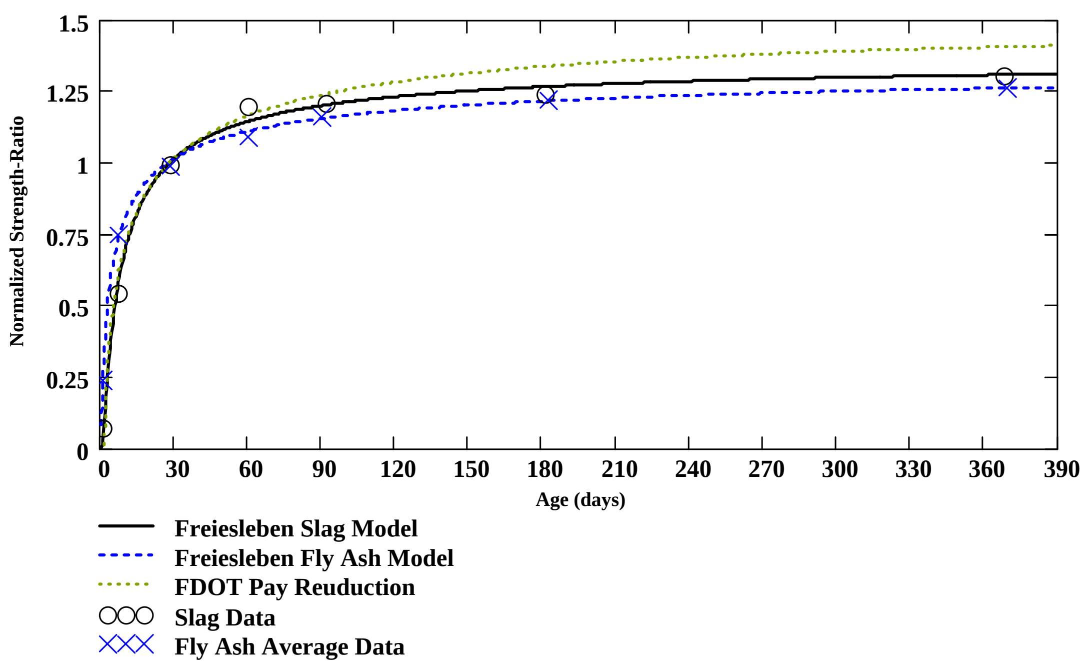

Figure 4.18: Comparison of Freiesleben Fly Ash and Slag Models for Type II Cement Mixes

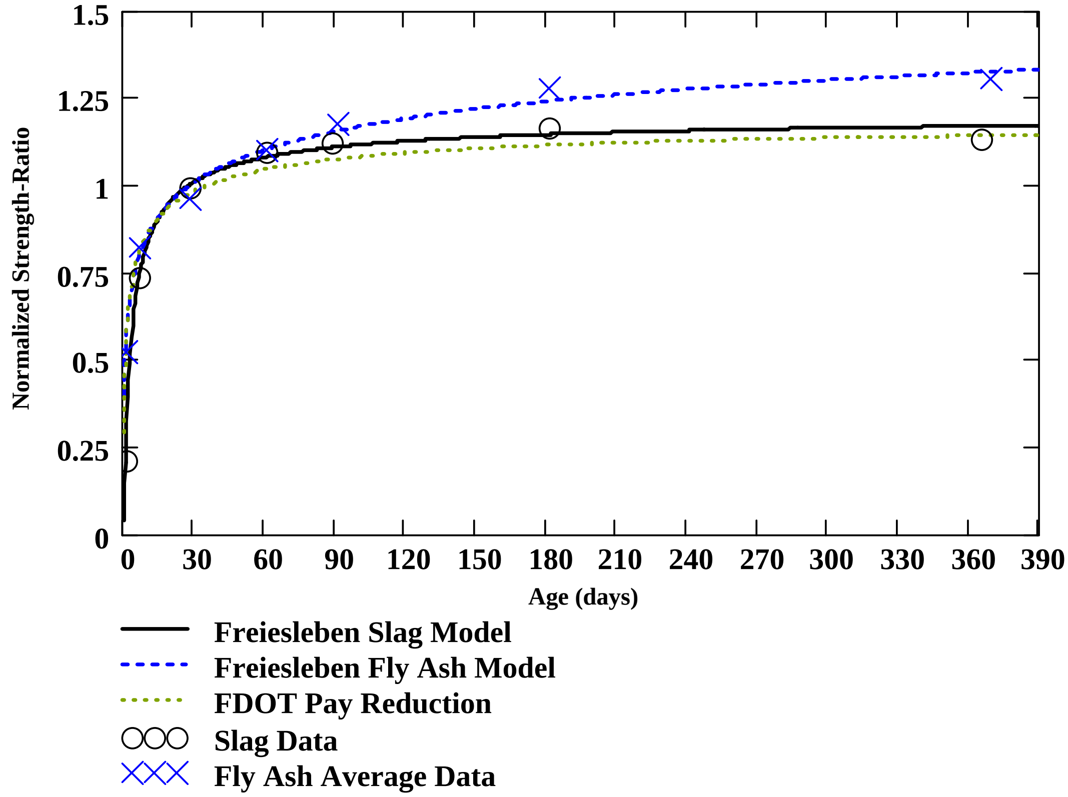

Figure 4.19: Comparison of Freiesleben Fly Ash and Slag Models for Type III Cement Mixes

Comparison of the plots of the Freiesleben fly ash and slag models and data in Figs. 4.17 through 4.19 show noticeable differences. For both Type I and Type III cement batches, the slag strength-ratio models fall below the fly ash models both before and after 28 days. For Type II cement batches, the slag model falls above the fly ash model after 28 days of ages. The differences in curing effects between fly ash and slag mixes are likely to increase at later ages. Therefore, separate strength-ratio models are needed for the fly ash and slag mixes.

The graphical comparison between the slag mix data and the FDOT pay reduction models plotted in Figs. 4.17 through 4.19 along with the large standard error of estimate from Table 4.4 show the inadequacy of the FDOT pay reduction equations in representing such data. Therefore, time-dependent strength variation in concrete with Gr. 100 slag may not be accurately represented by the current FDOT equations.

CHAPTER 5

RESULTS AND ANALYSIS OF MODULUS OF ELASTICITY DATA

5.1. Test Results

The results from the MOE tests are presented in Table 5.1, along with approximate age, corresponding compressive strength and unit weight. The data is sorted according to coarse aggregate type. The ranges of compressive strengths and unit weights are from 859 psi to 8,432 psi and 140.8 to 150.3 pcf, respectively. The test strength range is inclusive of the FDOT concrete Classes I through V [FDOT 2004], which range from 3,000 to 6,500 psi.

Plots of the MOE data are shown in Figs. 5.1 through 5.6. Figure 5.1 shows the MOE values plotted against the compressive strength, segregated by coarse aggregate types. Also shown is the FDOT MOE relationship for Florida lime rock with a fixed unit weight of 145 pcf (Eq. 2.7). Figure 5.2 is a plot of MOE values against the unit weights, also segregated by aggregate types. Figures 5.3 and 5.4 are reproductions of Figs. 5.1 and 5.2 with the data from the 1989 University of Florida study superimposed [Amornsrivilai et al 1989]. Figures 5.1 and 5.3 show that the current FDOT MOE relationship underestimates the actual MOE values found in this and the UF study. Figure

Table 5.1: Modulus of Elasticity Data Sorted by Coarse Aggregate Type

Batch ID*	Approx. Age (days)	f'_c (psi)	Unit Weight (pcf)	MOE (x 10^6 psi)
1FB	1	2,009	143.0	3.453
1FB	7	3,671	143.0	4.327
1FB	28	5,192	142.2	4.542
1FB	90	6,009	141.4	4.640
1FB	365	6,862	142.2	4.855
2FB	1	859	141.4	2.939
2FB	7	4,460	141.9	4.212
2FB	28	5,631	141.9	4.570
2FB	90	6,320	141.6	4.802
2FB	365	6,442	141.6	5.127
3FB	1	2,809	140.8	3.580
3FB	7	4,488	140.8	5.686
3FB	28	5,422	140.8	4.618
3FB	90	6,464	140.8	4.764
3FB	365	6,637	140.8	5.130
1FG	1	1,400	143.1	3.854
1FG	7	3,216	143.1	4.596
1FG	28	4,734	143.1	4.629
1FG	90	5,852	143.1	5.304
1FG	365	6,905	143.1	6.099
2FG	1	1,478	145.6	3.879
2FG	7	3,721	145.6	4.839
2FG	28	5,378	145.6	5.161
2FG	90	6,533	145.6	5.461
2FG	365	7,267	145.6	5.720
3FG	1	2,360	147.4	4.459
3FG	7	4,066	147.4	5.277
3FG	28	4,721	147.4	5.161
3FG	90	5,804	147.4	5.479
3FG	365	6,878	147.4	6.185
1FC	1	2,012	145.3	4.389
1FC	7	3,769	145.3	6.570
1FC	28	5,197	145.3	6.353
1FC	90	6,545	145.3	6.400
1FC	365	7,664	145.3	6.886
2FC	1	1,873	149.1	4.909
2FC	7	4,927	149.1	6.474
2FC	28	6,299	149.1	6.644
2FC	90	7,543	149.1	7.040
2FC	365	8,432	149.1	7.496
3FC	1	3,260	150.3	5.721
3FC	7	4,670	150.3	6.488
3FC	28	5,322	150.3	6.714
3FC	90	6,747	150.3	6.930
3FC	365	7,455	150.3	7.786

*Batch ID:

1st character: cement (Types I, II and III)
2nd character: mineral admixture (F: fly ash)
3rd character: aggregate (B: Brooksville, G: river gravel, C: Calera)

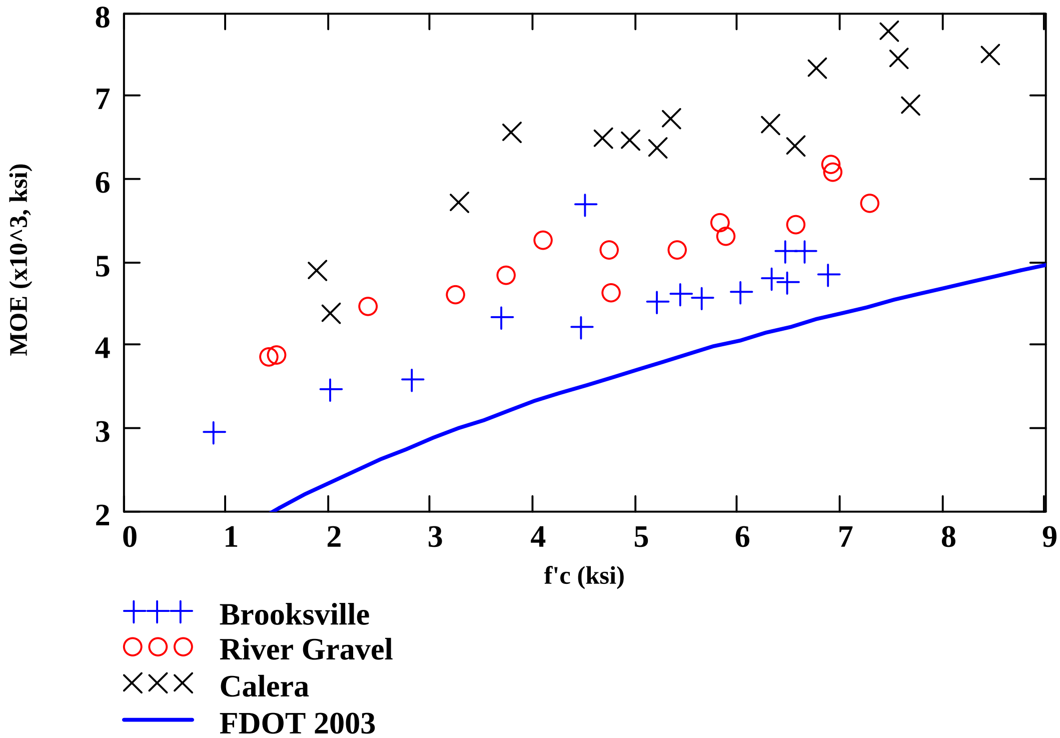

Figure 5.1: MOE versus Compressive Strength Data for Various Aggregate Types [FDOT 2003]

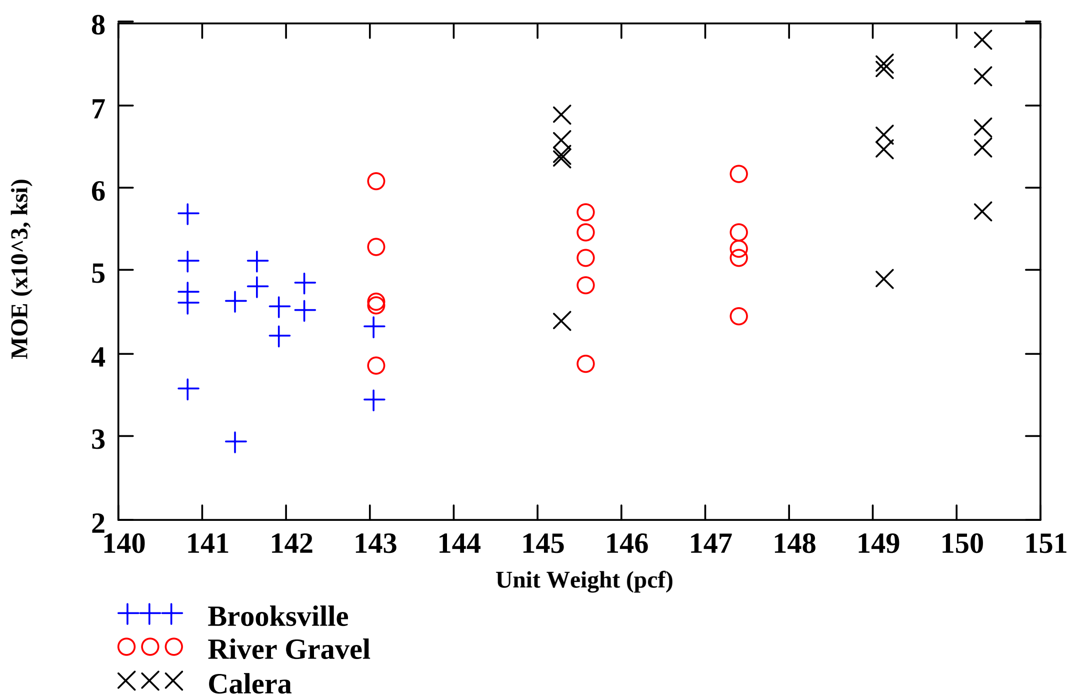

Figure 5.2: MOE versus Unit Weight Data for Various Aggregate Types

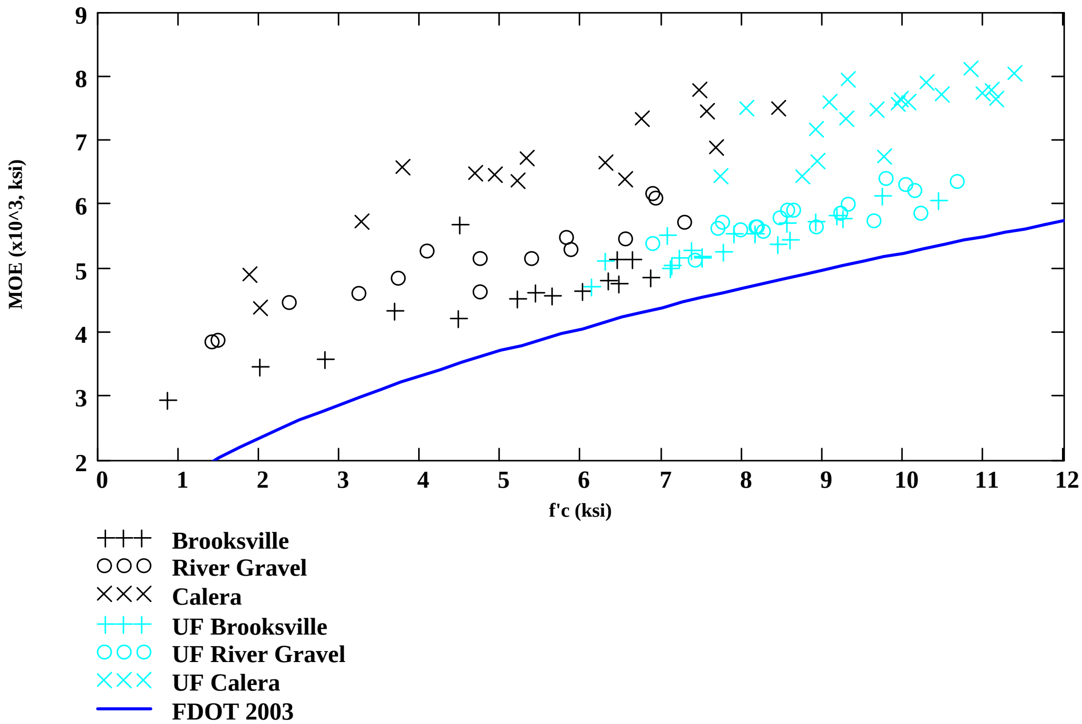

Figure 5.3: MOE versus Compressive Strength Data for Various Aggregate Types with UF Data [Amornsrivilai 89, FDOT 2003]

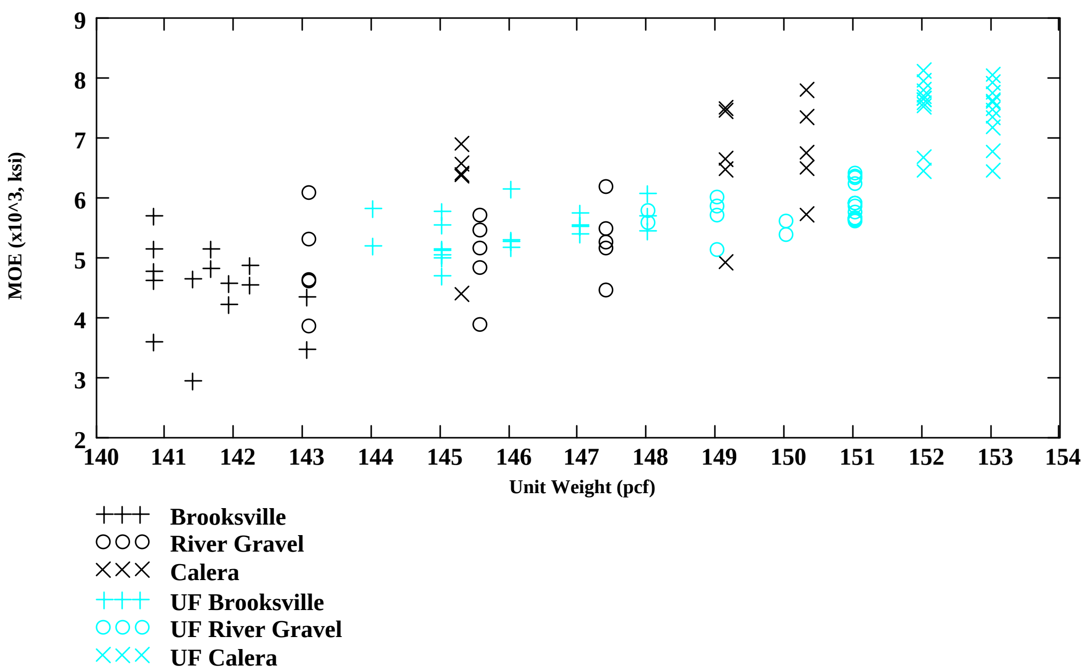

Figure 5.4: MOE versus Unit Weight Data for Various Aggregate Types with UF Data [Amornsrivilai 89]

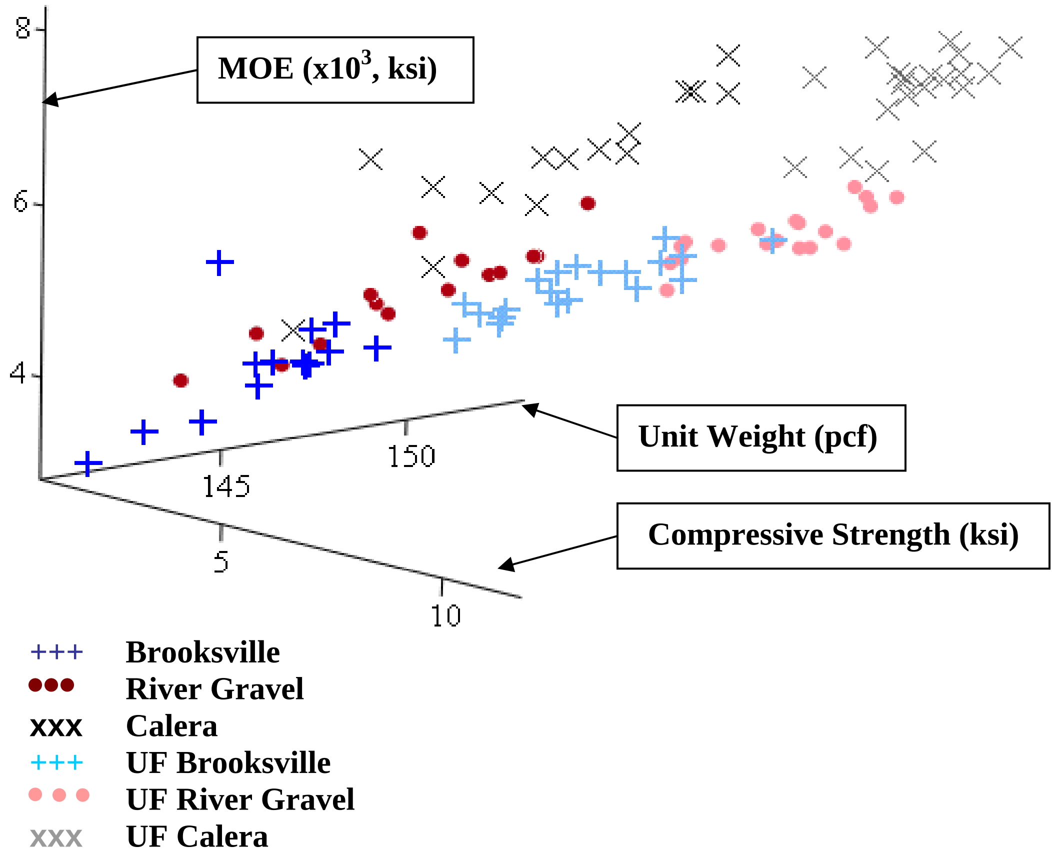

Figure 5.5: 3-D Plot of MOE versus Compressive Strength and Unit Weight Data

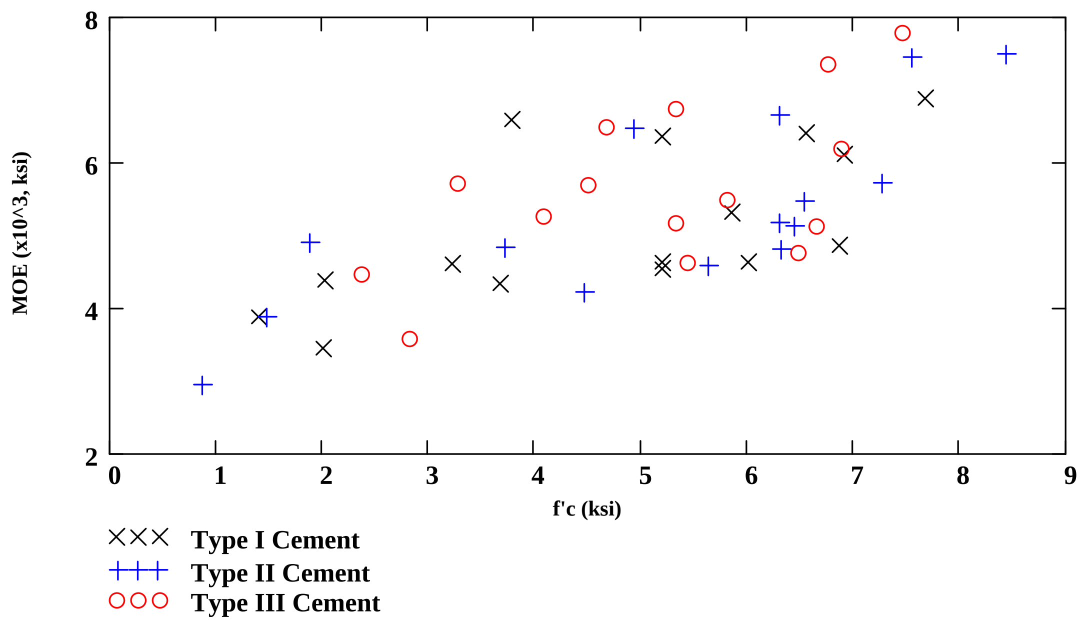

Figure 5.6: MOE versus Compressive Strength Data, Segregated by Cement Types

5.5 is a 3-D plot of MOE values versus compressive strength and unit weight with the UF data included. The UF data were included in the plots for comparison purposes only. However, they were not included in the final MOE models developed herein. Figure 5.6 is a plot of MOE values versus compressive strengths, segregated by cement types.

The two main factors affecting the MOE are the w/c ratio, which affects the compressive strength, and the aggregate used, which largely affects the unit weight [Mehta 1986]. Figure 5.1 clearly shows banding of the MOE data points for the same aggregate type. Data for the Brooksville lime rock fall in the bottom band, followed by the river gravel data in the middle band and the Calera lime rock data in the highest band. Table 3.4 shows that Calera aggregate has the largest specific gravity, followed sequentially by river gravel and Brooksville aggregates. It is apparent that the aggregate densities play a key role in the banding of the MOE data points. The respective aggregate densities affect the unit weight of the concrete. Figure 5.2 shows that the MOE data points for the different aggregates are generally grouped together in respective unit weight ranges. Figure 5.3 more clearly shows the aggregate banding of the MOE data points with the incorporation of the UF data. At higher ranges of compressive strength, the MOE data for various aggregates from this study tend to merge with the UF data. Figure 5.4 shows that the UF MOE data points for the different aggregates are also grouped together in respective unit weight ranges.

It is not possible to show the 3-D relationship of MOE, compressive strength and unit weight data on two-dimensional graphs such as Fig. 5.1-5.4. Two-dimensional plots can only show two parameters, greatly limiting the visualization of the relationships. The 3-D plot of Fig. 5.5 more powerfully shows these inter-relationships among the three parameters. The figure clearly shows the banding of the MOE data for the same aggregate type. It can be observed in Fig. 5.5 that the MOE data for Brooksville and river gravel aggregates are banded close together, and all the MOE data bands are narrow. It is apparent that there are clear distinctions among the MOE data for various aggregates, beyond what is represented by the 2-D plots shown earlier.

No clear pattern or banding of the MOE data points based on cement type is apparent. This is expected and supports previous claims that cement type plays no direct role in affecting MOE prediction [ACI 225R-99].

5.2 Regression Analysis

5.2.1 Resulting Equations and Errors

Regression analysis was performed on the MOE, compressive strength and unit weight data obtained in this study in order to develop MOE prediction models. The base model used by ACI 318 (Eq. 2.2), FDOT (Eq. 2.7) and Cook (Eq. 2.20) is as follows:

$$\boldsymbol{E_c = a.w^b \, . \, f'^{\,c}_c} \tag{5.1}$$

Where:

E_c = Modulus of Elasticity

w = unit weight of concrete

f_c = concrete compressive strength

a, b, c = variables

This base model was selected herein for the regression analysis procedure to develop appropriate MOE equations. By taking the natural log of both sides of Eq. 5.1, a linearized form of the equation was obtained to which multivariate regression analysis could be applied. The linearized form of Eq. 5.1 is as follows:

$$\boldsymbol{ln(E_c) = ln(a) + b.ln(w) + c.ln(f'_c)} \tag{5.2}$$

Various options for optimization of Eq. 5.2 are presented in Table 5.2. The first option was to optimize all three variables $\boldsymbol{a}$, $\boldsymbol{b}$ and $\boldsymbol{c}$ to determine the most accurate prediction of the MOE. The second option was to set $\boldsymbol{a}$ equal to unity and only optimize $\boldsymbol{b}$ and $\boldsymbol{c}$. This resulted in a simpler but less accurate MOE model. Options 3 through 6 were combinations of the variables optimized, with remaining variables fixed to current specifications. The last option was re-application of Option 1 analysis to the combined data from this study and the 1989 University of Florida study [Amornsrivilai et al 1989]. This option was performed for comparison purposes only.

As explained in Section 4.2.3, the commonly used R^2 value is not applicable to non-linear regression analysis needed for the MOE data. Although the linearized form (Eq. 5.2) of Eq. 5.1 was used to perform regression analysis, the R^2 value is not valid since the natural log form was used [Bates 1988, Myers 1986, Wetherill 1986]. Therefore, the standard error of estimate was used to assess the quality of fit of the MOE models (Eq. 4.1) [Triola 1998]. Table 5.3 presents the optimized resulting variables with standard errors. Various existing models for MOE prediction from the literature were examined for their applicability to the MOE data gathered in this study. The examined

Table 5.2: Various MOE Regression Optimization Options (Eq. 5.2)

Option	Details	Comments
1	All 3 variables (***a, b, c***) optimized.	Most accurate option
2	Both ***b*** and ***c*** optimized, with ***a*** = 1.0.	Second most accurate option
3	Only ***a*** optimized, with ***b*** = 1.5 and ***c*** = 0.5	Similar to the FDOT 2003 model (Eq. 2.7)
4	Both ***a*** and ***b*** optimized, with ***c*** = 0.5	----
5	Only ***b*** optimized, with ***a*** = 30 and ***c*** = 0.5	Similar to the FDOT 2003 model (Eq. 2.7)
6	Both ***a*** and ***c*** optimized, with ***b*** = 0	Eliminates unit weight as a predictor
7	Similar to Option 1, applied to the combined FAMU-FSU and UF data.	----

Table 5.3: Optimization Results for Various MOE Regression Options

Option	Optimized Variable			Variable Held Constant	Standard Error ($x10^{-3}$)
	a	b	c		
1	1.45×10^{-7}	5.8	0.28	None	471
2	1	2.64	0.28	a	613
3	43.7	1.5	0.5	b, c	809
4	6.66×10^{-7}	5.12	0.5	c	670
5	30	1.58	0.5	a, c	812
6	403,000	0	0.305	b	855
7	1.65×10^{-3}	4.08	0.189	None	737

Table 5.4: Variables and Standard Error of Estimates for Existing MOE Models

Model	Equation No.	Variables			Standard Error ($x10^{-3}$)
		a	b	c	
GFH-Texas	2.20	1	2.55	0.315	956
Tarmac-FL	2.21	325,300	0	0.305	1,401
FDOT	2.7	30	1.5	0.5	1,918
ACI 318	2.2	33	1.5	0.5	1,582
ACI 363	2.17	$E = 40{,}000 \cdot f'^{0.5}_c + 10^6$			1,844

Table 5.5: Aggregate Based Option 2 MOE Models

Option	Aggregate Type	Optimized Variables			Variables Held Constant
		a	b	c	
2-B	Brooksville	0.89	2.64	0.28	b, c
2-G	River Gravel	0.94	2.64	0.28	b, c
2-C	Calera	1.1	2.64	0.28	b, c

models, their respective parameter, and standard errors for their application to the MOE data are presented in Table 5.4.

Results for Option 1 (Table 5.3) show an unusually small value for ***a*** and a value for exponent ***c*** that is closer to ⅓ than ½ (the ACI and FDOT value). The variables for Option 2 application are fairly similar to those from the GFH-Texas model (Eq. 2.20). The general similarities between the obtained parameters for the FAMU-FSU and UF combined data, and those from Option 1, support the validity of Option 1. One optimized form of the current FDOT model (Option 3) resulted in a modification of the variable ***a*** from 30 to 43.7, reducing the error from 1,918 to 809. The other optimized form of the current FDOT model (Option 5) increased the unit weight exponent to 1.58 from 1.5, reducing the error from 1,918 to 812. Both Options 3 and 5 perform equally well in representing concrete MOE and improvising on the current FDOT MOE model. The current ACI-318 MOE model results in a high error, although slightly lower than the current FDOT model. The error for the current FDOT approach was approximately four times that of Option 1. Option 6 is only dependent on the compressive strength as the predictor variable, and results in an exponent for the strength that is close to ⅓.

The Tarmac-FL model developed by Cook (Eq. 2.21) for Pennsuco aggregate concrete showed a significant level of error, although the model was a better fit to the overall MOE data as compared to the current FDOT and the ACI 318 MOE models. All seven MOE models developed in this study performed better than the Tarmac-FL model for the data generated herein.

5.2.2. Graphical Comparison and Assessment

Plots of Options 1 and 2 cannot be shown on two-dimensional figures because the models are multivariate. They must either be shown on a 3-D plot, which would be difficult to represent in a single frame, or as a plot of the predicted MOE versus the actual MOE data. Plots of predicted MOE versus actual MOE were used herein to graphically show the quality of fit for Options 1 and 2. Options 1 and 2 were chosen herein because they resulted in the least standard error. The compressive strengths and unit weights for various data points were entered into the Options 1 and 2 MOE expressions to yield a list of predicted MOE values. The predicted MOE data was then plotted against the actual MOE data for comparison. Proximity of the data points to the line "Actual MOE = Predicted MOE" signifies accuracy of the predictor model.

Figures 5.7 and 5.8 show predicted MOE versus actual MOE plots for Options 1 and 2 MOE models, respectively, segregated by aggregate types. Figure 5.9 shows Options 1 and 2 data plotted on the same graph for comparison of fit. Predicted MOE versus Actual MOE data for the current FDOT model along with the Option 1 plots are presented in Fig. 5.10. Figure 5.11 presents Options 1 and 2 MOE models plotted against the MOE vs. compressive strength data for the various aggregate types. The relative similarity of accuracy of the two options is apparent from this figure.

Figures 5.7 and 5.8 reveal that Options 1 and 2 MOE model predictions for the Calera batches are too low, whereas predictions for Brooksville and river gravel batches are slightly high. Figures 5.7 through 5.9 show that Option 1 has a slightly better fit than Option 2 to the test data. Figure 5.10 shows that the current FDOT MOE approach clearly

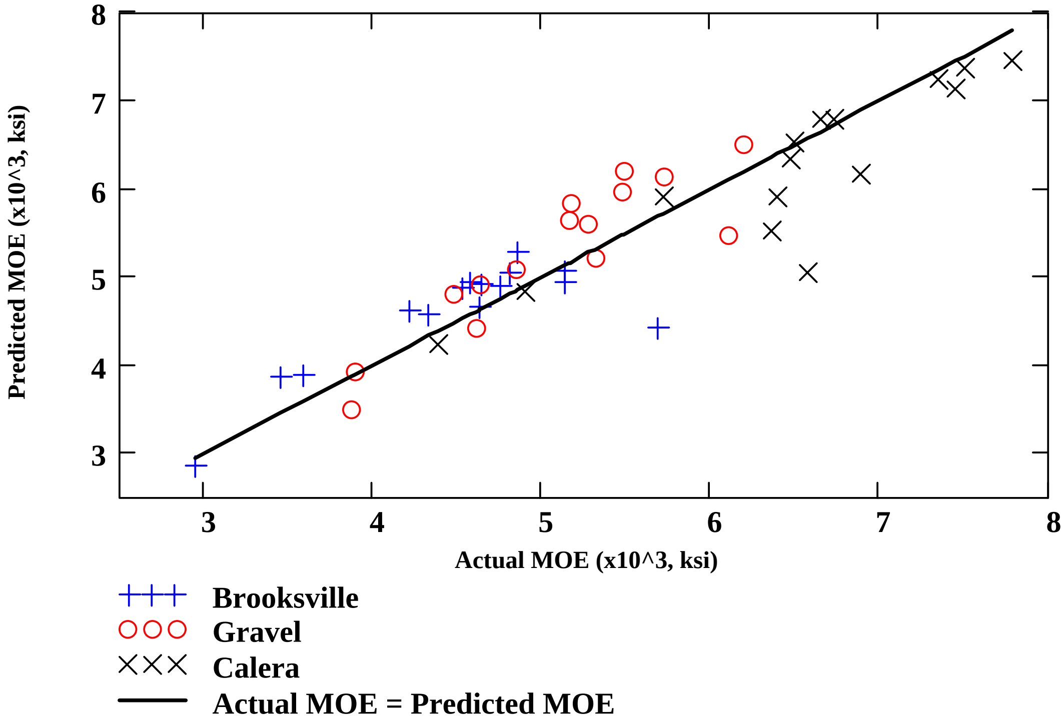

Figure 5.7: Predicted versus Actual MOE Segregated by Aggregate Types, Option 1 Model

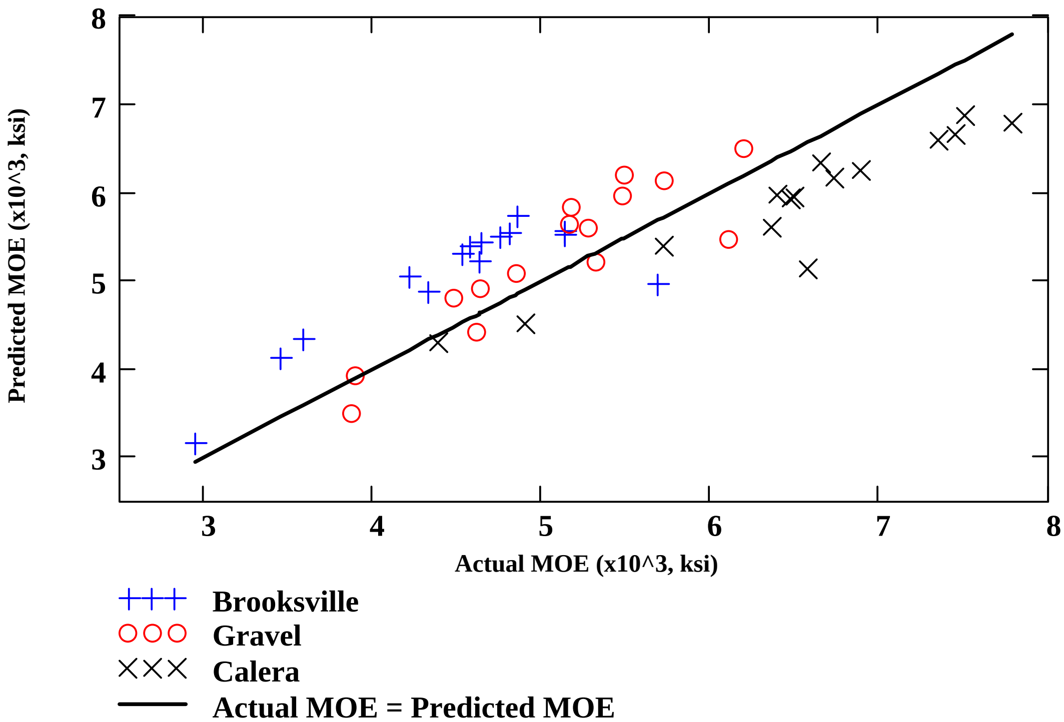

Figure 5.8: Predicted versus Actual MOE Segregated by Aggregate Types, Option 2 Model

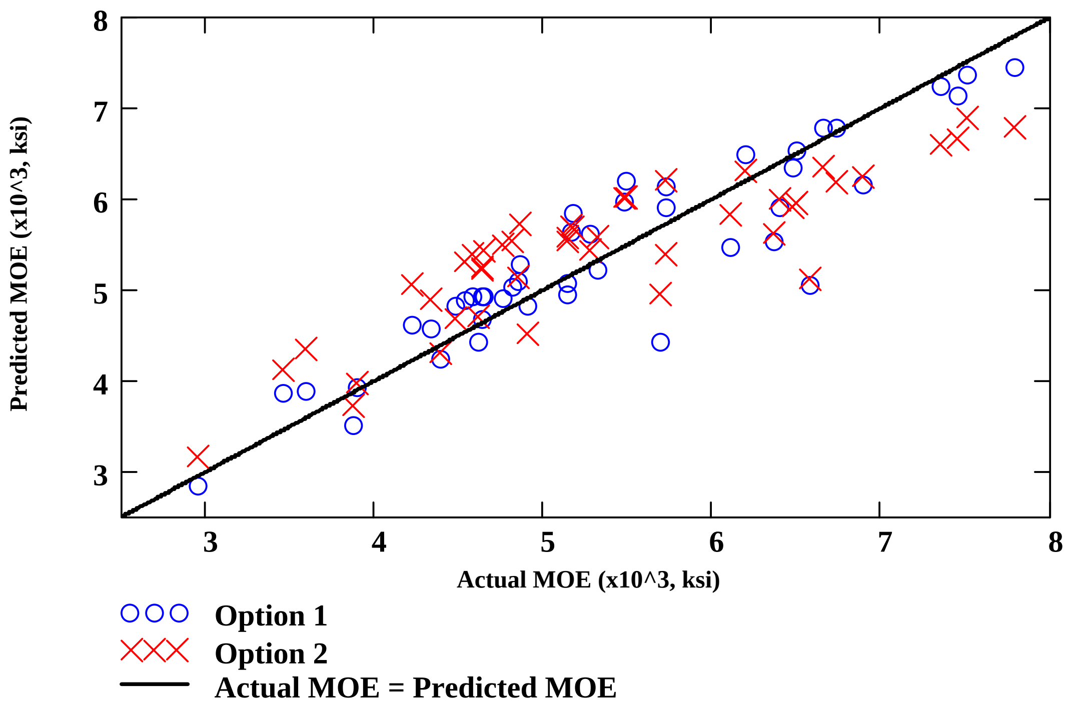

Figure 5.9: Predicted versus Actual MOE, Options 1 and 2 Models

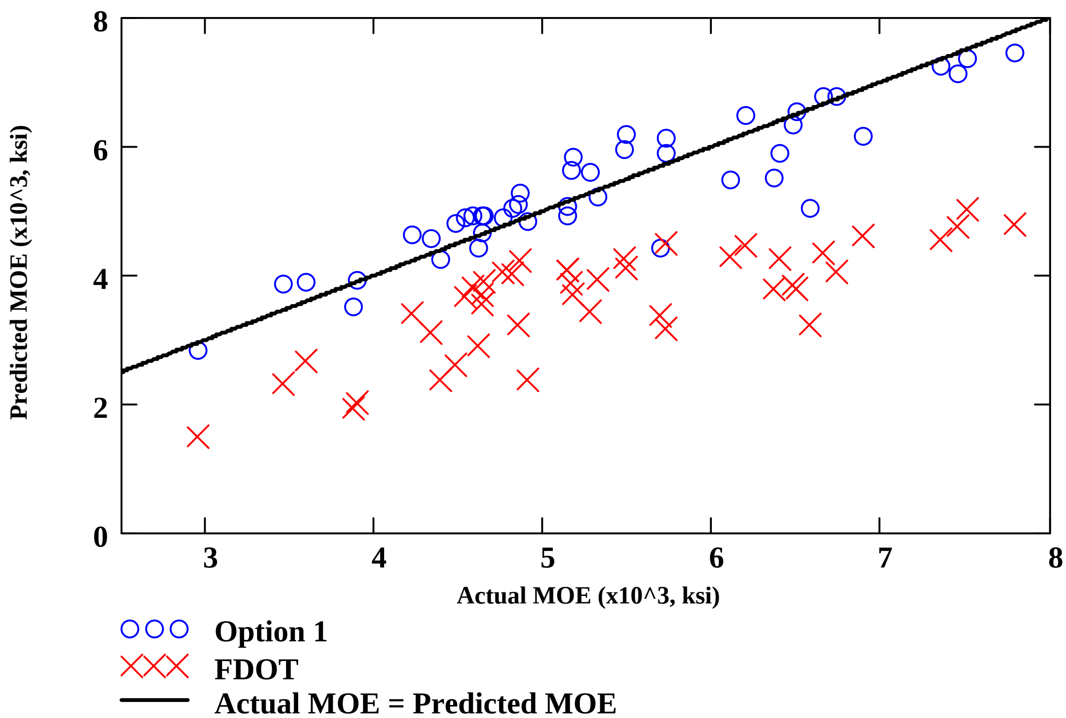

Figure 5.10: Predicted versus Actual MOE, Option 1 and FDOT 2003 Models

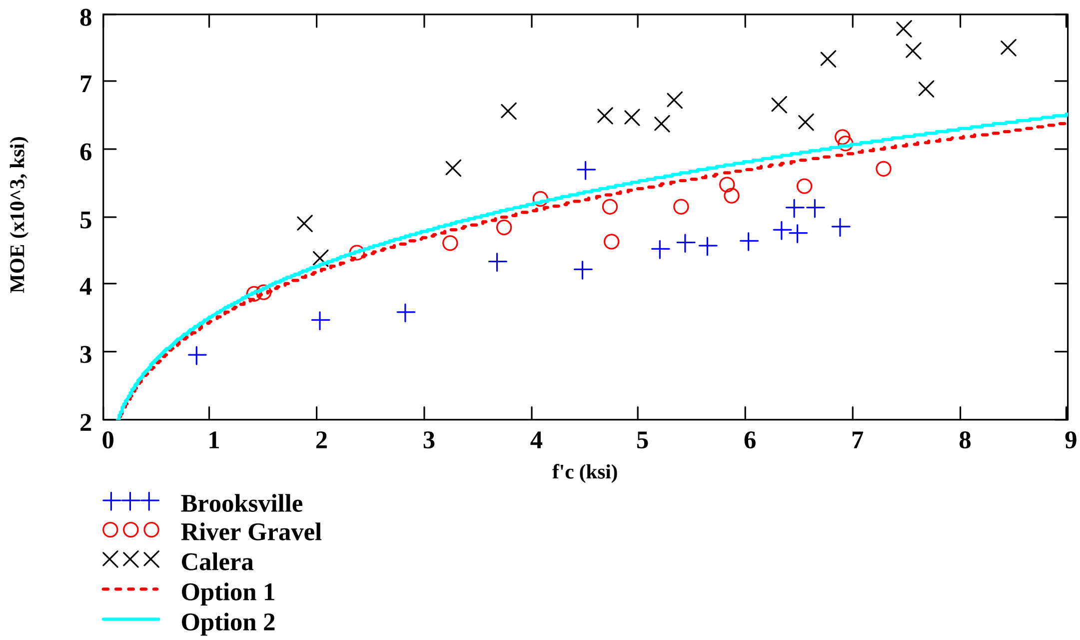

Figure 5.11: Option 1 and 2 MOE Models with Actual MOE Data

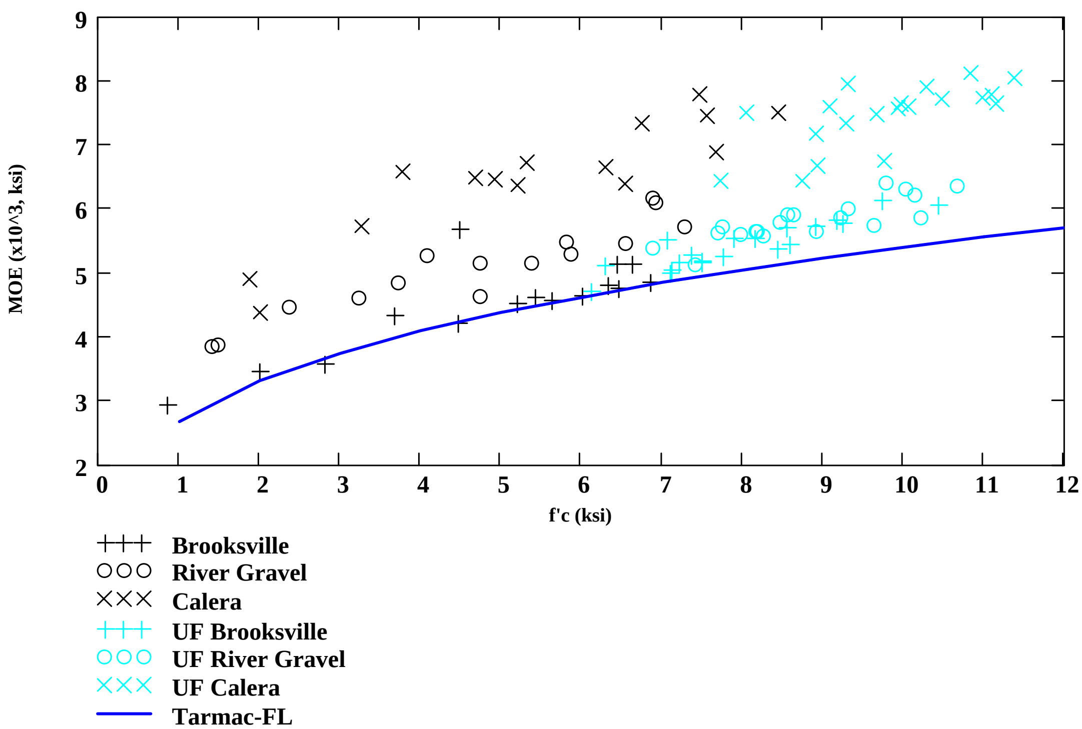

Figure 5.12: Tarmac-FL MOE Model Fit to Aggregate Based Data

underestimates the actual MOE data. Based on the high error of the FDOT approach from Table 5.4, and the plots of Figs. 5.1, 5.3 and 5.10, it may be inferred that the FDOT prediction is inadequate and too conservative in predicting the current FDOT concrete MOE.

Figure 5.12 shows that the Tarmac-FL model significantly under-predicts most of the MOE data generated in this study and the UF study. This is because the model is based on MOE data from Florida concrete using mostly Pennsuco limerock aggregate, which has a low specific gravity. Concrete with denser aggregates such as Calera were not included in the MOE data base. It is noteworthy that the Tarmac-FL equation shows a good fit to the MOE data for concrete with Brooksville aggregate from this study.

An examination of Table 5.3 shows that Option 1 results in the best fit with the smallest error of all models considered herein. Option 2 is the second best MOE model; this model is simpler to use than the Option 1 model. The error for Option 2 is approximately 1.3 times that of Option 1. However, the Option 2 model is less sensitive to variations in the unit weight due to its lower value of the unit weight exponent ***b***. This means that even though Option 1 is the best MOE model for the range of unit weights from this study, Option 2 may be a better predictor of MOE for unit weights outside the range. The exponent ***c*** for both options is equal, signifying that the variations in compressive strengths will have a similar impact on both models. It should be noted that both options are only valid for the range of data presented in this study. Use of either option to extrapolate MOE values for compressive strengths or unit weights outside of these ranges should be performed with caution.

5.2.3 Aggregate Based MOE Models

Figures 5.3 and 5.5 clearly show the banding of MOE data points for the three aggregate types used, i.e., for Brooksville, river gravel and Calera aggregates. Therefore, a single MOE equation representing data from the three aggregate types (Options 1-2 from Table 5.2) may not be sufficiently accurate for individual aggregate types. An inspection of Figs. 5.7 and 5.8 shows that the MOE Options 1 and 2 models developed herein for the combined aggregate type data under-predict the MOE for Calera data, over-predict the MOE for the Brooksville data, and slightly under-predict the river gravel data. Table 3.4 shows that the specific gravity of the Calera aggregate (2.72) is the greatest of the 3 aggregates considered herein, followed in sequence by the river gravel (2.63) and the Brooksville aggregates (2.43). The dense Calera aggregate produces stiff concrete with higher MOE values than the other two aggregates. The sequence of the MOE data bands in Figs. 5.3 and 5.5 follow the relative densities of the three aggregates.

It may be appropriate to utilize a modification factor for various aggregate types, to be applied to the combined MOE models developed herein. Towards this end, the Option 2 MOE model presented in Table 5.3 was applied individually to each of the three aggregate based MOE data sets. The regression analyses were performed with the variables ***b*** and ***c*** being held constant at the previously obtained values of 2.64 and 0.28, respectively. The objective was to calibrate Option 2 MOE model for the three aggregate types, producing a single aggregate based modifier ***a***. The resulting MOE model options 2-B, 2-G and 2-C for the Brooksville, river gravel and Calera aggregate data are presented in Table 5.5. The aggregate based multiplier ***a*** for the three aggregate types are 0.89, 0.94 and 1.1, respectively. These multipliers need to be applied to the generic

Option 2 MOE model for the three aggregate types. The three developed aggregate based MOE models are plotted in Fig. 5.13, together with the generic Option 2 model. In the plots of Fig. 5.13, the actual average unit weights of 141.6, 145.3 and 148.2 pcf were used as input to the respective Brooksville, river gravel and Calera MOE models for clarity of plotting. The excellent fit of the aggregate based MOE models to the individual aggregate based data bands is obvious.

AASHTO Subcommittee on Bridges and Structures is now considering a revision to the standard equation for MOE that will introduce an aggregate factor into the equation, where the factor for type of aggregate is to be taken as 1.0, unless determined by physical tests. The current FDOT MOE equation is based on a similar approach with a factor of 0.90. All of the values provided in the FDOT MOE table in the Structures Design Guideline are 90% of the ACI predicted values for all unit weights listed.

If AASHTO adopts the proposed revision, it will appear in the AASHTO LRFD Bridge Design Specifications in 2005. The idea of the aggregate based MOE factor was developed as part of an NCHRP research project on Prestress Losses in High Strength Concrete Bridge Girders.

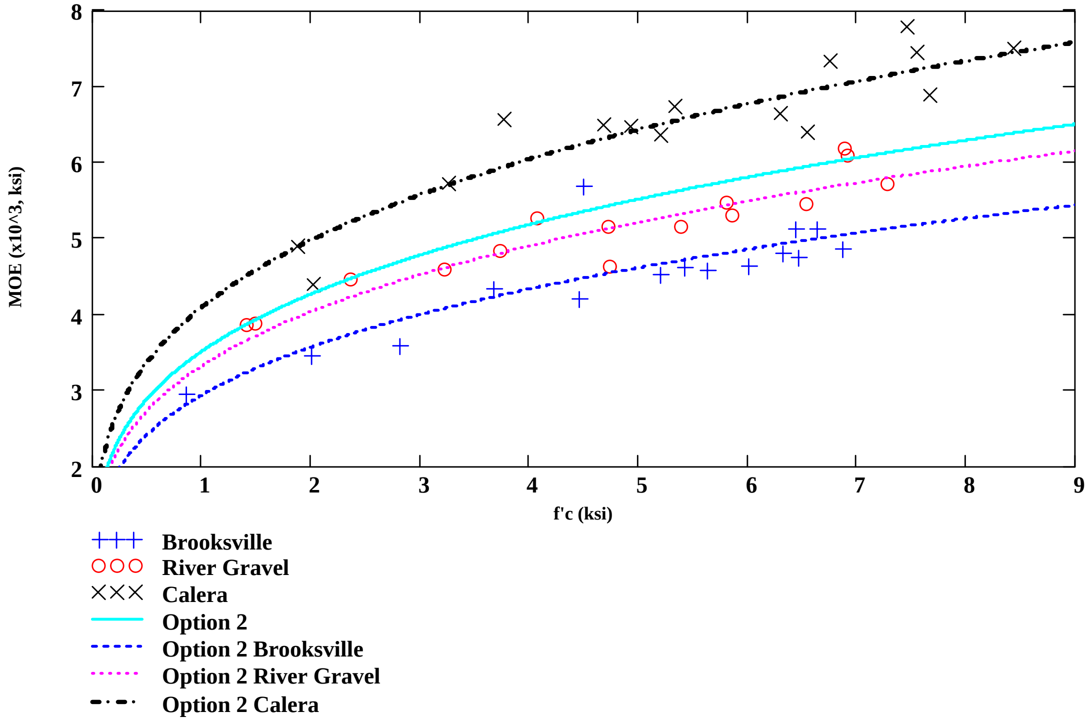

Figure 5.13: Aggregate Based Option 2 MOE Models with Actual MOE Data

CHAPTER 6

CONCLUSIONS AND RECOMMENDATIONS

The following conclusions and recommendations are made based on the results of this study:

1. Appropriate existing models available in the literature may be conveniently used to represent the time dependent variation of compressive strength of FDOT concrete. Regression analyses are conveniently used to adopt the existing models after proper calibration, and to gauge the relative quality of fit of each model.
2. The current FDOT compressive strength pay reduction models are not adequate to represent time dependent compressive strength variations in FDOT concrete, as compared to the applicability of several other models from literature. The Freiesleben, the CEB-FIP and the Hyperbolic models all perform significantly better than the FDOT pay reduction models in representing the variation of compressive strength of FDOT concrete with time. The standard error of fit for the FDOT pay reduction models is about three times that for the Friesleben models.
3. Among the models considered herein, the Friesleben model performs best in the prediction of time-dependent compressive strength of typical FDOT concrete using

20% Class F fly ash, and Types I, II and III cements. The Friesleben fly ash concrete models developed herein are as follows:

Cement Type I $$f_c(t) = 2.04 \cdot e^{-\left(\frac{8.31}{t}\right)^{0.276}} \cdot f'_c(28) \tag{6.1}$$

Cement Type II $$f_c(t) = 1.37 \cdot e^{-\left(\frac{2.89}{t}\right)^{0.514}} \cdot f'_c(28) \tag{6.2}$$

Cement Type III $$f_c(t) = 2.07 \cdot e^{-\left(\frac{5.38}{t}\right)^{0.191}} \cdot f'_c(28) \tag{6.3}$$

Based on the developed models, the 28-day concrete compressive strength prediction models for fly ash concrete, based on core strengths, are as follows:

Cement Type I $$f'_c(28) = 0.490 \cdot e^{\left(\frac{8.31}{t}\right)^{0.276}} \cdot f'_c\left(t\right) \tag{6.4}$$

Cement Type II $$f'_c(28) = 0.730 \cdot e^{\left(\frac{2.89}{t}\right)^{0.514}} \cdot f'_c\left(t\right) \tag{6.5}$$

Cement Type III $$f'_c(28) = 0.483 \cdot e^{\left(\frac{5.38}{t}\right)^{0.191}} \cdot f'_c\left(t\right) \tag{6.6}$$

4. The time dependent variation of FDOT fly ash concrete was found to be significantly different than the FDOT slag concrete. Therefore, separate models are needed to

represent such slag concrete data. The Hyperbolic Model was found to have the best fit to the slag concrete time dependent behavior, followed closely by the Friesleben model. To be consistent with the fly ash concrete model chosen, the Freiesleben model may be selected to predict the time-dependent compressive strength of concrete using 50% Grade 100 slag, and Types I, II and III cements, as follows:

Cement Type I $$f_c(t) = 1.26 \cdot e^{-\left(\frac{7.06}{t}\right)^{1.06}} . f'_c(28) \tag{6.7}$$

Cement Type II $$f_c(t) = 1.37 \cdot e^{-\left(\frac{6.02}{t}\right)^{0.747}} . f'_c(28) \tag{6.8}$$

Cement Type III $$f_c(t) = 1.21 \cdot e^{-\left(\frac{2.36}{t}\right)^{0.672}} . f'_c(28) \tag{6.9}$$

The corresponding prediction models for the 28-day strength of slag concrete, based on the strength found at time "t" are:

Cement Type I $$f'_c(28) = 0.794 \cdot e^{\left(\frac{7.06}{t}\right)^{1.06}} . f'_c(t) \tag{6.10}$$

Cement Type II $$f'_c(28) = 0.730 \cdot e^{\left(\frac{6.02}{t}\right)^{0.747}} . f'_c(t) \tag{6.11}$$

Cement Type III $$f'_c(28) = 0.826 \cdot e^{\left(\frac{2.36}{t}\right)^{0.672}} \cdot f'_c(t) \qquad (6.12)$$

For convenience of users the time dependent compressive strength ratio variation with time of FDOT concrete is presented in Table 6.1. It is recommended that the developed models for slag concrete should be used for a concrete age of 28 days and beyond. The models for slag concrete may predict inaccurate compressive strength for the concrete of early ages.

5. Various Modulus of Elasticity (MOE) models from existing literature may be conveniently applied and calibrated to represent FDOT concrete MOE.
6. Previous MOE data collected at the University of Florida for the three aggregate types studied in this report compliment well the data generated herein, and validates the test results.
7. The current FDOT MOE model significantly under-predicts the MOE of various FDOT concrete types. Other recent MOE models such as the GFH-Texas and the Tarmac-FL models also under-predict the MOE data generated in this study.
8. Density and specific gravity of the coarse aggregate significantly affect the MOE of FDOT concrete. Distinct bands of aggregate based MOE values are clearly apparent in MOE plots developed herein.
9. Development of prediction models for the MOE of FDOT concrete with an overall combined data set, as functions of compressive strength and unit weight, resulted in two desirable and accurate models, as follows:

Table 6.1: Relative Strength Development of Concrete As a Percentage of 28-day Compressive Strength

Concrete Age (days)	Results of $F = \frac{f'_c(t) \times 100}{f'_c(28)}$		
	Type I Cement	**Type II Cement**	**Type III Cement**
Fly Ash Concrete			
1	33.94	24.40	52.14
7	71.52	72.62	79.99
28	99.82	100.35	99.80
90	121.56	115.48	115.47
180	133.03	121.55	124.14
365	143.52	126.06	132.43
Slag Concrete			
1	0.045	3.00	20.40
7	45.91	56.06	74.79
28	99.85	99.75	100.14
90	117.74	119.97	111.03
180	121.94	126.58	114.66
365	124.04	130.75	117.04

Option 1: $$E_c = 1.45 \cdot 10^{-7} \cdot w^{5.8} \cdot f'_c{}^{0.28} \qquad (6.13)$$

Option 2: $$E_c = w^{2.64} \cdot f'_c{}^{0.28} \qquad (6.14)$$

Option 1 was found to be the most accurate of all options considered, for the range of compressive strength and unit weights considered in this study. Option 2 was found to be the next best model, which is simpler and has a form similar to the current FDOT and ACI MOE models. However, Option 2 is less sensitive to variations in unit weight due to a smaller exponent of the unit weight. These two equations are valid for compressive strengths in the range of 859 to 8,432 psi and unit weights in the range of 140.8 to 150.3 pcf.

10. The Option 2 generic MOE model may be modified through the application of aggregate based modification factors developed in this study. The modification factors for Brooksville, river gravel and Calera aggregates are: 0.89, 0.94 and 1.1, respectively.
11. Further research with different sources of cement and mineral admixtures may improve the accuracy of the models developed herein. Data addition from tests performed beyond 12 months age will also be useful in extending the data range. Accuracy of the models may be improved with addition of data from different concrete classes and variations in coarse aggregate types.

APPENDIX

Table A.1: Base Concrete Design Mix

Issued	: D. B. Bagwell	Date	: 04/04/1990
Reviewed:	J. R. Ward	Mix No.	: 07-0004

Class Concrete: IV VIB (5500 psi)

Source of Materials

Coarse Aggregate	: Florida Mining & Materials	Grade :	57 S.G. (SSD): 2.430
Fine Aggregate	: Florida Mining & Materials	F.M. :	2.10 S.G. (SSD): 2.630
Pit No. (Coarse)	: 08-005	Type :	Crushed Limestone
Pit No. (Fine)	: 16-081	Type :	Silica Sand
Cement	: Florida Mining & Materials	Spec :	AASHTO M-85 Type II
Air Entr. Admix	: Darex W. R. Grace	Spec :	AASHTO M-154
1st Admix	: WRDA 79 W. R. Grace	Spec :	AASHTO M-194 Type D
2nd Admix	: ---	Spec :	---
3rd Admix	: ---	Spec :	---
Fly Ash	: Florida Mining & Materials	Spec :	ASTM C-618 Class F

Hot Weather Mix

Cement (lb)	: 576	Slump Range	: 1.50 to 4.5 in
Coarse Agg (lb)	: 1700	Air Content	: 2.0 % to 6.0 %
Fine Agg (lb)	: 1000	Unit Weight (wet)	: 137.6 pcf
Air Ent Admx (oz)	: 6.0	w/c Ratio (Plant)	: 0.41 lb/lb
1st Admixture (oz)	: 43.0	w/c Ratio (Field)	: 0.41 lb/lb
2nd Admixture (oz)	: 0.0	Theo Yield	: 27 cu ft
3rd Admix (oz)	: 0.0		
Water (gal)	: 35.40		
Water (lb)	: 295.0		
Fly Ash (lb)	: 144		

Producer Test Data

Chloride Cont	: ---
Slump	: 3.25 in
Air Content	: 4.00 %
Temperature	: 89 deg (F)
28 day Compressive Strength (psi)	: 6570

Table A.2: Final Concrete Mix Proportions

Batch ID*	Cement (lb/yd^3)	Fly Ash or Slag (lb/yd^3)	w/c ratio	Water (lb/yd^3)	Coarse Aggregate (lb/yd^3)	Sand (lb/yd^3)	Type A Admixture (oz)	Air Entraining Admixture (oz)
1FB	576	144	0.42	305	1714	1000	28.7	6.0
2FB	576	144	0.41	295	1715	1001	28.7	6.0
3FB	576	144	0.43	312	1702	997	28.7	6.0
1FG	576	144	0.38	274	1849	1001	28.7	6.0
2FG	576	144	0.35	253	1848	1000	28.7	4.0
3FG	576	144	0.39	282	1842	997	28.7	4.0
1FC	576	144	0.51	369	1912	1001	28.7	6.0
2FC	576	144	0.41	295	1911	1000	28.7	6.0
3FC	576	144	0.40	290	1906	997	28.7	4.2
1SB	360	360	0.43	308	1725	1010	28.7	6.0
2SB	360	360	0.42	299	1724	1010	28.7	2.0
3SB	391	391	0.40	311	1682	985	28	2.0

*Batch ID:

1st character: cement (Types I, II and III)
2nd character: mineral admixture (F: fly ash, S: slag)
3rd character: aggregate (B: Brooksville, G: river gravel, C: Calera)

Table A.3: Compressive Strength Data Normalized Using Freiesleben Model

Batch Name	Target Age (day)	Cement Type I Actual Age (day)	I Strength Ratio	II Actual Age (day)	II Strength Ratio	III Actual Age (day)	III Strength Ratio
FB	1	1.12	0.388	1.00	0.148	0.99	0.501
	7	7.00	0.709	7.23	0.777	6.93	0.801
	28	28.08	1.002	28.33	0.973	27.86	0.968
	60	60.00	1.160	59.98	1.055	59.73	1.087
	90	89.94	1.160	90.62	1.092	92.06	1.154
	180	181.00	1.290	186.64	1.141	179.94	1.222
	365	367.88	1.325	373.72	1.113	375.83	1.185
FG	1	1.03	0.301	1.01	0.279	1.00	0.487
	7	7.31	0.691	6.85	0.703	7.04	0.839
	28	28.15	1.017	28.20	1.016	28.10	0.974
	60	60.18	1.130	60.09	1.078	61.02	1.097
	90	90.14	1.257	89.79	1.235	90.81	1.197
	180	181.92	1.400	179.95	1.297	182.81	1.285
	365	365.26	1.483	368.07	1.373	364.86	1.419
FC	1	1.00	0.383	1.02	0.288	0.99	0.572
	7	7.21	0.717	7.15	0.757	7.00	0.820
	28	28.87	0.989	29.24	0.968	27.94	0.934
	60	60.92	1.161	59.78	1.135	60.98	1.116
	90	88.86	1.245	89.87	1.159	89.95	1.184
	180	180.70	1.360	180.07	1.214	179.87	1.326
	365	364.98	1.458	364.83	1.296	365.02	1.308
SB	1	1.03	0.139	0.99	0.072	1.01	0.211
	7	7.36	0.482	7.04	0.544	7.05	0.737
	28	28.36	1.001	28.24	0.996	27.99	0.993
	60	60.31	1.137	60.27	1.196	60.91	1.096
	90	90.07	1.195	92.20	1.208	89.10	1.124
	180	179.95	1.218	180.99	1.241	180.94	1.164
	365	373.04	1.233	368.07	1.306	365.02	1.133

*Batch ID:
1st character: cement (Types I, II and III)
2nd character: mineral admixture (F: fly ash, S: slag)
3rd character: aggregate (B: Brooksville, G: river gravel, C: Calera)

LIST OF SUPPORTING INDUSTRIES

The following industries and personnel donated materials and provided valuable advice for this research.

Don Patterson, Jim Davenport, and Paul Owen
Cemex

Allen Barenthin
Rinker USA

Billy Dickens
W. R. Grace

Jerry Rose
Lafarge Corporation

Werner Krupp
Florida Fly-Ash

Chuck Washington
Vulcan Materials

David Herndon
Martin Marietta

To Dr. P. Kumar Mehta:

I am completing a thesis at Florida State University entitled "*Time Dependent Strength and Elasticity Development in Florida Concrete*." I would like your permission to reprint in my thesis excerpts from the following:

Mehta, P. Kumar, *Concrete Structure, Properties, and materials*, Prentice Hall, 1986

This report is also to be submitted to the Florida Department of Transportation. The requested permission extends to any future revisions and editions of my thesis, including non-exclusive world rights in all languages. These rights will in no way restrict republication of the material in any other form by you or by others authorized by you. Your signing of this letter will also confirm that you own [or your company owns] the copyright to the above-described material. If these arrangements meet with your approval, please sign this letter where indicated below and return it to me in the enclosed return envelope. Thank you very much.

Sincerely,

Shuler Bryant McKinnie

S. Bryant Mckinnie

PERMISSION GRANTED FOR THE
USE REQUESTED ABOVE:

PKmehta (P.K. Mehta)

Date: 9/20/02 Prof. of Civil Engineering
U.C. Berkeley, CA. 94720

REFERENCES

AASHTO LRFD Bridge Design Specifications. American Association of State Highway and Transportation Officials. 2nd Edition - 2003 Interim Revisions, Washington, D.C. 2003.

ACI 209R-92. ACI Committee 209, *Prediction of Creep, Shrinkage, and Temperature Effects in Concrete Structures*, American Concrete Institute, Farmington Hills, MI. 1992.

ACI 221R-96. ACI Committee 221, *Guide for Use of Normal Weight and Heavyweight Aggregates in Concrete*, American Concrete Institute, Farmington Hills, MI. 1996.

ACI 225R-99. ACI Committee 225, *Guide to the Selection and Use of Hydraulic Cements*, American Concrete Institute, Farmington Hills, MI. 1999.

ACI 232.2R-96. ACI Committee 232, *Use of Fly Ash in Concrete*, American Concrete Institute, Farmington Hills, MI. 1996.

ACI 233R-03. ACI Committee 233, *Slag Cement in Concrete and Mortar*, American Concrete Institute, Farmington Hills, MI. 2003.

ACI 318-02. ACI Committee 318, *Building Code Requirements for Structural Concrete (318-02) and Commentary (318R-02)*. 2002.

ACI 363R-92. ACI Committee 363, *State-of-the-Art Report on High-Strength Concrete*, American Concrete Institute, Farmington Hills, MI. 1992.

Amornsrivilai, P., Bloomquist D., Dobson, E., Meletiou, C. A., Richardson, D., Shih, C., and Tia, M. *Extension of Field and Laboratory Study of Modulus of Rupture and Permeability of Structural Concrete in Florida*. State Project No. 99700-7479-010. University of Florida, Gainesville, FL. 1991.

Amornsrivilai, P., Bloomquist, D., Dobson, E., Meletiou, C. A., Richardson, D., Shih, C., Tia, M., and Yang, M. C. K. *Extension Study of Field and Laboratory Study of Modulus of Rupture and Permeability of Structural Concrete in Florida for Development of a Concrete Performance Specification*, State Project No. 99700-7387-119. University of Florida, Gainesville, FL. 1992.

Amornsrivilai, P., Bloomquist, D., Dobson, E, Meletiou, C. A., Richardson, D., Soongswang, P., Tia, M., and Yang, M. C. K. *Field and Laboratory Study of Modulus of Rupture and Permeability of Structural Concretes in Florida*, State Project No. 99700-7387-119. University of Florida, Gainesville, FL. 1989.

ASTM C 39-03. *Standard Test Method for Compressive Strength of Cylindrical Concrete Specimens*, Annual Book of ASTM Standards, vol. 04.02, West Conshohocken, PA. 2003.

ASTM C 127-01. *Standard Test Method for Density, Relative Density (Specific Gravity), and Absorption of Coarse Aggregate*, Annual Book of ASTM Standards, vol. 04.02. West Conshohocken, PA. 2003.

ASTM C 128-01e1. *Standard Test Method for Density, Relative Density (Specific Gravity), and Absorption of Fine Aggregate*, Annual Book of ASTM Standards, vol. 04.02. West Conshohocken, PA. 2003.

ASTM C 138/C 138M-01a. *Standard Test Method for Density (Unit Weight), Yield, and Air Content (Gravimetric) of Concrete*, Annual Book of ASTM Standards, vol. 04.02. West Conshohocken, PA. 2003.

ASTM C 143/C 143M-03. *Standard Test Method for Slump of Hydraulic Cement Concrete*, Annual Book of ASTM Standards, vol. 04.02. West Conshohocken, PA. 2003.

ASTM C 173/C 173M-01e1. *Standard Test Method for Air Content of Freshly Mixed Concrete by the Volumetric Method*, Annual Book of ASTM Standards, vol. 04.02. West Conshohocken, PA. 2003.

ASTM C 192/C 192M-02. *Standard Practice for making and Curing Concrete Test Specimens In the Laboratory*, Annual Book of ASTM Standards, vol. 04.02. West Conshohocken, PA. 2003.

ASTM C 260-01. *Standard Specification for Air-Entraining Admixtures for Concrete*, Annual Book of ASTM Standards, vol. 04.02. West Conshohocken, PA. 2003.

ASTM C 494/C 494M-04. *Standard Specification for Chemical Admixtures for Concrete*, Annual Book of ASTM Standards, vol. 04.02. West Conshohocken, PA. 2003.

ASTM C 469-02. *Standard Test Method for Static Modulus of Elasticity and Poisson's Ratio of Concrete in Compression*, Annual Book of ASTM Standards, vol. 04.02. West Conshohocken, PA. 2003.

ASTM C 566-97. *Standard Test Method for Total Evaporable Moisture Content of Aggregate by Drying*, Annual Book of ASTM Standards, vol. 04.02. West Conshohocken, PA. 2003.

ASTM C 618-03. *Standard Specification for Coal Fly Ash and Raw or Calcined Natural Pozzolan for Use as a Mineral Admixture in Concrete*, Annual Book of ASTM Standards, vol. 04.02. West Conshohocken, PA. 2003.

ASTM C 642-97. *Standard Test Method for Density, Absorption, and Voids in Hardened Concrete*, Annual Book of ASTM Standards, vol. 04.02. 1999.

ASTM C 918-02. *Standard Test Method for Measuring Early-Age Compressive Strength and Projecting Later-Age Strength*, Annual Book of ASTM Standards, vol. 04.02. West Conshohocken, PA. 2003.

ASTM C 989-99. *Standard Specification for Ground Granulated Blast-Furnace Slag for Use in Concrete and Mortars*, Annual Book of ASTM Standards, vol. 04.02. West Conshohocken, PA. 2003.

ASTM C 1064/C 1064M-03. *Standard Test Method for Temperature of Freshly Mixed Portland Cement Concrete*, Annual Book of ASTM Standards, vol. 04.02. West Conshohocken, PA. 2003.

ASTM C 1074-98. *Estimating Concrete Strength by the Maturity Method*, Annual Book of ASTM Standards, vol. 04.02. West Conshohocken, PA. 2003.

ASTM C 1231/C 1231M-00e1. *Standard Practice for Use of Unbonded Caps in Determination of Compressive Strength of hardened Concrete Cylinders*, Annual Book of ASTM Standards, vol. 04.02. West Conshohocken, PA. 2003.

Bates, D., Watts, D. *Nonlinear Regression analysis and its Applications*. John Wiley & Sons, Inc. 1988.

Cain, C. *Fly Ash in Concrete Pipe*, Concrete Pipe News, vol. 31, No. 6, pg. 114-116, Dec, 1979.

Carino, N. J. and Malhorta, V. M. *CRC Handbook on Nondestructive Testing of Concrete*. CRC Press LLC. 1991.

CEB-FIP Model Code 1990, Final Draft, CEB Bulletin D'Information, No. 203, pp. 39-52, 1990.

Chin, F. K. *Relation Between Strength and Maturity of Concrete*, Journal of the American Concrete Institute, 68(3), 196. 1971.

Cook, James E. *10,000 psi Concrete*, Concrete International, Design and Construction. vol. 11, No. 10, pp. 67-75. Oct 1989.

Cook, James E. On going research effort at Tarmac Florida, Inc. on Modulus of Elasticity. 2004.

De Larrard, F., Le Roy, R., and Pons, G. *The AFREM code type model for creep and shrinkage of high performance concrete*, Proceedings of the Fourth International Symposium on Utilization of High-Strength/High-Performance Concrete. Vol. 2, Paris, France. pp. 387-396. 1996.

FDOT. *Florida Department of Transportation Standard Specifications for Road and Bridge Construction*. 2004.

FDOT. *Florida Department of Transportation Structures Design Guidelines for Load and Resistance Factor Design*. August, 2003.

Freiesleben, H. P., and Pederson, E. J. *Curing of Concrete Structures*, CEB Information Bulletin 166. May, 1985.

Han, N. *Time Dependent Behavior of High Strength Concrete*. Delft University Press. 1996.

Jin, Y., Yazdani, N. *Substitution of Fly Ash, Slag, and Admixtures in FDOT Mix Designs*. Contract No. BC-352-3. 2001.

Klieger, P., and Isberner, A. W. *Laboratory Studies of Blended Cement—Portland Blast-Furnace Slag Cements*, Journal - PCA Research and Development Department Laboratories. vol. 9, No. 3, pp. 2-22. Sept, 1967.

Lew, H. S., and Reichard, T. W. *Prediction of Strength of Concrete from Maturity, Accelerated Strength Testing*, SP-56, American Concrete Institute, 229. 1978.

Mehta, Kumar P. *Concrete Structure, Properties, and Materials*. Prentice Hall. 1986.

Myers, Raymond H. *Classical and Modern Regression with Applications*. PWS Publishers. 1986.

Nykanen, A. *Hardening of Concrete at Different Temperatures, Especially Below the Freezing Point*, Proceedings, RILEM Symposium on Winter Concreting, Danish Institute for Building Research Copenhagen, Session BII. 1956

Pauw, A. *Static Modulus of Elasticity of Concrete as Affected by Density*, Journal of the American Concrete Institute. pp. 679-687. Dec 1960.

Plowman, J. M. *Maturity and the Strength of Concrete*, Mag. concr. Res., 8(22), 13. 1956.

Rens, K. L. *Concrete Maturity: A Quantitative Understanding of How Early-Age Temperatures Affect the Maturity Concept*. NSF #: Civil and Mechanical Systems (CMS) 9988584. 2004.

Triola, M. F. *Elementary Statistics 7th Edition*. Addison Wesley Longman, Inc. 1998.

Wetherill, Barrie. *Regression Analysis with Applications*. Chapman and Hall. 1986.